

Nowcasting using regression on signatures

Samuel N. Cohen^{1,2}, Giulia Mantoan⁴, Lars Nesheim^{2,3,5}, Áureo de Paula³, Arthur Turrell^{4,6}, and Lingyi Yang^{1,2}

¹University of Oxford

²The Alan Turing Institute

³University College London, Cemmap and Institute for Fiscal Studies

⁴Bank of England

⁵University of Bristol

⁶No.10 Downing Street

December 17, 2025

Abstract

We introduce a new method of nowcasting using regression on path signatures. Path signatures capture the geometric properties of sequential data. Because signatures embed observations in continuous time, they naturally handle mixed frequencies and missing data. We prove theoretically, and with simulations, that regression on signatures subsumes the linear Kalman filter and retains desirable consistency properties. Nowcasting with signatures is more robust to disruptions in data series than previous methods, making it useful in stressed times (for example, during COVID-19). This approach is performant in nowcasting US GDP growth, and in nowcasting UK unemployment.

Keywords: nowcasting, signatures

Disclaimer: Any views expressed are solely those of the author(s) and do not represent those of the Bank of England or its policy committees, or of No.10 Downing Street. This paper should therefore not be reported as representing the views of the Bank of England or UK government. We are grateful for seminar and conference participants at the 37th IARIW General Conference (2022), 2022, 2023, 2024 ESCOE Conference, the 2022 CFE-CMStatistics Conference, 2023 SIAM Conference on Financial Mathematics and Engineering, the 2023 Royal Economic Society Conference, the 2023 Financial Econometrics workshop, the 2023 Workshop on Nowcasting at Paris School of Economics, the 10th International Congress on Industrial and Applied Mathematics (2023), the 2024 Conference on Real-Time Data Analysis, Methods, and Applications, the 2024 Econdat Conference, the 2024 Society for Nonlinear Dynamics and Econometrics Conference, The 2024 British Applied Mathematics Colloquium, 2024 ECONDAT. The authors gratefully acknowledge the ONS-Turing Strategic partnership for funding. L.Y. was supported by EPSRC [EP/S026347/1] and the Hong Kong Innovation and Technology Commission (InnoHK Project CIMDA). SC was supported by the UKRI Prosperity Partnership Scheme (FAIR) under EPSRC Grant [EP/V056883/1]. For the purpose of open access, the authors have applied a CC BY public copyright licence to any Author Accepted Manuscript (AAM) version arising from this submission.

1 Introduction

Policymakers need up-to-date economic information to make decisions. However, the collection and compilation of the data underlying key economic indicators takes time. For example, the first estimate of UK monthly GDP is published approximately 6 weeks after the end of the month it pertains to. Alternative indicators that have a shorter publication lag, or that are released more frequently, offer the opportunity to glean information about the economy in close to real-time and so inform policy in a timely manner. For instance, the UK’s Office for National Statistics publishes a range of weekly alternative indicators of economic activity covering card spending, retail footfall, and more.

Models that can harness these alternative indicators to produce estimates of *current* economic activity – whether it be gross domestic product (GDP), employment or other official statistics – are known as nowcasting models, and their predictions are called nowcasts. As an example, a nowcasting model might combine a range of alternative indicators and output an estimate of the GDP figure for the current month, in contrast to a forecast, which looks ahead to activity which has not yet occurred.

The economic literature on nowcasting has grown dramatically in the past 20 years (e.g. see Stock and Watson, 2002; Giannone et al., 2006; Bok et al., 2018), and has focused on three challenges that arise when attempting to use a large and varied set of contemporaneous indicators for real-time insights on the economy. The first is how we incorporate data into a model when there are missing observations from mixed or irregular sampling frequencies. The second is how we extend beyond linear time-invariant systems to allow for time-varying parameters or for non-linearity. Third and finally, there is a challenge in how to incorporate large numbers of predictors into a single model, i.e. imposing structure to reduce the dimensionality of the problem.

During roughly the same time period, a set of tools to model non-linear multidimensional time series has been developed in the mathematics and machine learning literature (see Section 3.3 for further details). These tools model time series as continuous time “paths” and extract low dimensional representations of these paths known as “signatures”. It has been shown that path signatures perform well in prediction tasks (Graham, 2013; Morrill et al., 2020), suggesting that signatures can provide a tool to address the three nowcasting challenges.

Building on these developments, in this paper, we introduce a new nowcasting method, regression on signatures, that addresses all three of the nowcasting challenges in new and powerful ways: regression on signatures is compatible with standard dimension reduction tools, handles missing observations and mixed frequencies, and requires minimal additional effort when inferring non-linear relationships. Path signatures are compatible with dimension reduction tools because they are features extracted from data that can be treated like any other variables. They handle mixed frequencies and missing data because they effectively model time series in continuous time and capture the interactions between features in which the ordering of events is preserved (Gyurkó et al., 2013; Levin et al., 2013). Finally, signatures are able to infer non-linear relationships because they are non-linear features with universal representation properties (Lyons et al., 2007) and, as with state-space models, signatures can be used in non-stationary

settings.

An additional key advantage of regression on signatures is the transparency of its estimation, particularly when compared to other next-generation nowcasting approaches that leverage deep learning. While machine learning can yield strong predictive performance, their underlying models are often high-dimensional and non-linear, making it difficult to interpret estimated relationships or assess robustness. Recent advances (e.g. SHAP values (Lundberg and Lee, 2017), counterfactual methods (Black et al., 2021)) have improved our ability to explain complex models, but these remain secondary layers of analysis rather than part of the estimation itself and can lack the transparency and simplicity of regression. In contrast, signature-based models rely on linear regression, for which the estimation procedures, sampling properties, and interpretation of coefficients are well-understood ¹. The linear structure of regression on signatures ensures that estimation remains transparent, stable, and amenable to standard inference techniques.

Using the path signature for nowcasting is very simple. First, we take available observations and compute their signature (the data points are treated as discrete observations of continuous paths). This can be done using any one of several free open source Python libraries that compute signatures, for example, `esig`, `iisignature` (Reizenstein and Graham, 2020), and `roughPy` (Morley and Lyons, 2024). Second, the computed signatures are used as regressors to predict the target variable of interest. This will be referred to as the *signature method* in the rest of the paper. The signature method can be combined with standard dimension reduction methods prior to the first step by e.g. extracting principal components before computing the signatures.

The introduction of the signature method for nowcasting is the primary contribution of this paper. This is an entirely new approach to nowcasting and has the aforementioned advantages relative to existing methods. Additionally, we show that the signature method provides superior performance on a standard problem in the literature, nowcasting US GDP, when compared to a direct application of Dynamic Factor Models (including the New York Federal Reserve’s Dynamic Factor Model described by Bok et al. (2018)). We also show that the signature method performs strongly when nowcasting UK unemployment changes, despite the challenging context of irregular information flows, multiple delays in the publication of the input and target variables due to external events (such as the COVID-19 pandemic), and a range of observation frequencies.

Our second contribution is to prove mathematically that the Kalman–Bucy filter can be written as a linear function of signatures. Put another way, signatures generalise linear Kalman filters, and recover the Kalman filter as a special case. In addition to our theoretical proof, we provide simulations that confirm estimates from the signature method do indeed match those of the Kalman filter.

This is a remarkable result: regression on signatures can capture any state-space model, even those with non-linear relationships, in any number of dimensions. Furthermore, using signatures as features eliminates some of the traditional complexity of time series modelling:

¹The signature terms themselves may be abstract, they do have a geometric interpretation (see Section 3.3)

choices over transformations and feature combinations matter far less because signatures provide ready-made features for generic input series. Because of these properties, this simple approach is applicable to a wide range of nowcasting tasks. The price for this flexibility is that the signature method can be high-dimensional, resulting in a need for substantial quantities of data or the use of dimension-reduction tools to prevent overfitting.

Our third contribution is to show how to combine signatures with standard dimension reduction techniques, like principal component analysis and dynamic factor models, so that the approach we introduce can be used in as wide a variety of settings as possible and can make use of large numbers of indicators effectively.

This paper contributes to the more recent literature on new methodologies to nowcast macroeconomic variables, including Jokubaitis et al. (2021), Proietti et al. (2021), Soybilgen and Yazgan (2021), Aastveit et al. (2018), Ankargren and Jonéus (2021), Babii et al. (2022), and on modeling missing data points and dimension reduction, such as Pellegrino (2020), Smeekes and Wijler (2021), Buccheri et al. (2021), and Chan et al. (2023) in a more general context than nowcasting.

2 Background on challenges in nowcasting

In this section, we discuss commonly occurring challenges for nowcasting in economics in more detail. We will address these challenges using the signature method in later sections.

2.1 Missing observations and mixed frequency or irregular sampling

Due to varying publication lags, delays, and interruptions, the time series for some variables entering a nowcasting model often have missing observations. When these missing observations affect the end of the observation window, this is often referred to as the “ragged-edge” problem (Wallis, 1986). The challenge is how to adapt standard discrete-time time-series methods to condition on arbitrary patterns of missing information. This can rapidly escalate into a complex programming challenge. Similarly, we would like to use all possible high-frequency variables (for example daily, weekly, or monthly data on prices, expenditure, or revenue) to predict low-frequency variables (such as monthly or quarterly GDP). This is the mixed frequency data problem. Again the challenge is how to combine these complex mixed frequency data.

Several solutions to these problems have been developed in the macroeconometrics literature. One option for the missing data problem is to use the classic discrete time Kalman filter (e.g. Kalman, 1960; Stock and Watson, 2002; Bańbura and Modugno, 2014). This approach assumes a linear time series structure and imputes missing values using the Kalman filter. We discuss this option in more detail in Section 3.

A second option to address both problems is to combine the bridge method (Schumacher, 2016) with imputation. The bridge method addresses the mixed frequency problem using a two-equation system, first aggregating the set of high-frequency predictors to produce low-frequency

predictors and then using the low-frequency predictors to predict the low-frequency target. We illustrate how bridge methods work via an example. Suppose we wish to use a single monthly variable z_t to predict a quarterly target y_t . One bridge model for this problem is

$$y_t = \sum_{s=1}^p \alpha_s y_{t-3s} + \beta_0 + \beta_1 x_t + \varepsilon_t \quad (1)$$

$$x_t = \sum_{s=0}^2 \gamma_s z_{t-s}. \quad (2)$$

Equation (1) is an autoregressive equation used to predict y_t , where p indicates the lag in the autoregressive process of the quarterly target and ε_t is an exogenous noise process. The parameters in Equation (1) are typically estimated from the data. Equation (2) is the “bridge” equation that aggregates the high-frequency variable to the same frequency as the low-frequency variable. The parameters in the bridge equation are typically chosen *ex ante*. For example, if x_t is the quarterly average of z_t , then $\gamma_s = \frac{1}{3}$ for all s .

The bridge equation addresses the mixed frequency problem. To overcome the ragged edges, missing values of z_t are imputed using an auxiliary forecasting model such as an AR(p) process

$$z_t = \delta_0 + \sum_{s=1}^p \delta_s z_{t-s} + \eta_t,$$

where η_t is a zero mean white-noise process, δ_0 and δ_s are parameters to be fitted.

For simple patterns of mixed frequency data (e.g. monthly predictors and quarterly targets), the bridge method is easy to use and does not require users to specify in detail the high frequency dynamics of the system. However, the aggregation method employed is ad hoc and likely needs to be adapted for different contexts. Moreover, adapting the method to more complicated patterns of mixed frequency data (e.g. combining weekly, monthly, or irregularly sampled data) can be challenging.

A third approach directly relates high-frequency indicators to a low-frequency target: this is the mixed data sampling (MIDAS) model (Ghysels et al., 2005). MIDAS accommodates data sampled at different frequencies by incorporating higher frequency variables using distributed lag terms with fractional lags. Mathematically, it can be written in a form that is very similar to the bridge equation; the distinction is that MIDAS employs a more general functional form than Equation (2) and its parameters are estimated rather than specified *ex ante*. An example of the MIDAS equation for a target y_t is:

$$y_t = \sum_{i=1}^{k_{lo}} a_i x_{i,t}^{lo} + \sum_{j=1}^{k_{hi}} b_j \sum_{k=0}^m w_j(k; \theta_j) \cdot x_{j,t-k}^{hi} + \varepsilon_t, \quad (3)$$

where y_t is the dependent variable, $x_{i,t}^{lo}$ are low-frequency predictors with coefficients a_i , $x_{j,t-k}^{hi}$ are high-frequency predictors with coefficients b_j , $w_j(k; \theta_j)$ are exponential Almon weights (Almon, 1965), and ε_t is the error term. The exponential Almon lag weight function is defined

by

$$w_j(k; \theta_j) = \frac{\exp(1 + s_k(\theta_{j1} + \theta_{j2}s_k))}{\sum_{k=0}^m \exp(1 + s_k(\theta_{j1} + \theta_{j2}s_k))},$$

where $s_k = k/m$ is the normalised lag position, θ_{j1} , θ_{j2} are the weight parameters for predictor j , and m is the maximum lag length. The exponential Almon lag avoids parameter proliferation when k_{hi} in Equation (3) is large.

The objective function used to estimate the coefficients in the MIDAS model is

$$\min_{a_i, b_j, \theta_j} \frac{1}{2} \sum_{t=1}^T (y_t - \hat{y}_t)^2,$$

where \hat{y}_t is the predicted value and the optimisation is subject to the constraints $\theta_{j1}, \theta_{j2} \geq 0 \forall j$. Non-linear optimisation solvers such as BGFS (Broyden, 1970; Fletcher, 1970; Goldfarb, 1970; Shanno, 1970) and L-BFGS-B (Byrd et al., 1995) can be used to find the coefficients.

To date, most empirical nowcasting studies using the methods above only deal with regularly sampled data with missing observations. This is because nowcasting typically uses official published data that are released on a regular schedule. However, in recent years there has been an increase in the use of alternative data sources, e.g. web-scraped data and supermarket scanner data. These alternative sources can be high-frequency, and have complicated or irregular missingness patterns. Furthermore, statistical offices have recently struggled with issues such as COVID-19 and declining survey response rates that have, at times, caused significant delays in publishing both input and target variables relevant to economic nowcasting.

Therefore, there is a need for a nowcasting methodology that can handle mixed frequency of arbitrary frequency, complex irregularly sampled data, and data with arbitrary patterns of missing values. Signature methods can handle all of these cases. We discuss these points in the sections below and illustrate our results with simulations and empirical applications.

2.2 Time-varying parameters and non-linearities

Classic time series methods, such as the autoregressive integrated moving average (ARIMA) model, assume that the dynamics of a low-dimensional variable, after suitable differencing to ensure stationarity, can be modelled by a linear model with autoregressive and moving average components. That is, after differencing, the data are stationary, the model is linear, and the parameters of the model are assumed to be constant. In nowcasting settings, all three of these assumptions can be restrictive – for example, when there are large shocks to the economy, which is also when it is critical to have an accurate guide to what is happening.

State-space models offer one approach to relax these restrictions (Durbin and Koopman, 2012). While the linear Kalman filter is the best known, state-space models in general are highly flexible and can allow for non-linearity and time-varying parameters. A common difficulty in using these methods is that the state-space representation needs to be specified, and cannot easily be learned from historical data. Many papers, including Hamilton (1994), Nielsen and Berg (2014), Carter and Kohn (1994), Kim et al. (1999), Kim (1994), also allow for time-varying parameters.

2.3 Dimension reduction

In most nowcasting exercises, a large number of indicators are used to predict a single target. For example, the Federal Reserve Bank of New York staff nowcasting model uses 37 variables to nowcast US GDP (FRBNY, 2016). The need to extract useful information from high-dimensional time series data has only increased as new indicators have become available. For instance, McCracken and Ng (2016) describes the St Louis Federal Reserve Monthly Database for Macroeconomic research, which contains 134 monthly US indicators.

The macroeconomic nowcasting literature has tackled dimensionality issues in a variety of ways. The leading approaches include dynamic factor models (DFMs), Bayesian vector autoregressions (BVARs), and penalised estimation methods like the LASSO.²

Dynamic factor models were introduced into economics by Geweke (1977) and are reviewed in Stock and Watson (2017) and Bai and Ng (2008). These models are based on the idea that most of the time series variation in a large set of economic indicators is driven by the dynamics of a small number of unobserved common factors. These factors can be estimated from the complete set of economic variables using singular value decomposition of the data matrix. The dynamics of the factors are analysed using standard time series methods such as vector autoregression. There has been rapid development of DFM methods in applied macroeconomic analysis, and they have been used extensively in economic forecasting and nowcasting (Giannone et al., 2006; Doz et al., 2006; Bok et al., 2018).

Bayesian vector auto-regressions (BVARs), developed for macroeconomics by Litterman (1979) and Sims (1980) (see Karlsson (2013) for a review), regularise and limit the dimensionality of models by first specifying informative prior beliefs on the parameter space and then using Bayesian methods to estimate the posterior distribution of the parameters. The posterior distribution is then used to nowcast the economic variables of interest. These methods are generally restricted to linear models, and so depend on careful choice of parameterisation. They also require care to ensure that the priors capture relevant information – for example momentum effects and non-stationarity typically need to be explicitly included.

Penalised estimation methods limit the dimensionality of models by including a penalty term in the estimation objective function. For example, the LASSO estimator, popularised in statistics by Tibshirani (1996), adds a penalty based on the sum of the absolute values of the parameters (known as the L1 penalty). This shrinks parameter estimates towards zero and, due to the non-smooth penalty function, selects only a subset of variables to have non-zero coefficients. The ridge estimator (Hoerl and Kennard, 1970) instead adds a penalty based on the sum of squares of the parameters (known as the L2 penalty). This also has the effect of shrinking parameter estimates towards zero. The Elastic Net (Zou and Hastie, 2005) combines the L1 and L2 penalties. Many other penalty function are possible. Penalised estimation allows researchers to include very large numbers of predictors in nowcasting models and, in many settings, improves the results of nowcasts by reducing over-fitting. These methods have been used in nowcasting in Babii et al. (2021), for example.

²Recent macroeconomics papers have also investigated the use of other machine learning methods including random forests and artificial neural networks (Richardson et al., 2021).

In Section 6, we show how to combine dynamic factor models with a signature method to produce nowcasts for US GDP growth. Unfortunately, we cannot directly compete with the NY Fed Nowcast given the restrictions over set of variables publicly available. However, on the same dataset, our DFM improves (Bok et al., 2018) nowcast’s accuracy by 20%.

3 Theory

In this section, we outline the underlying mathematical theory for nowcasting with state-space models and illustrate their connection to the path signature. We start with a recap of the discrete time Kalman filter and its continuous time extension, then introduce the theory of signatures, and finally show how regression on signatures subsumes the Kalman filter. We introduce here notation that we use throughout the paper.

3.1 Discrete time state-space models

First, we recap the classic discrete-time Kalman filter (see Bertsekas (2012) for an overview).

Suppose that we have a hidden process $Y \in \mathbb{R}^d$ that we cannot directly measure, but would like to infer from an observed process $X \in \mathbb{R}^m$. In the context of nowcasting, Y_t would be e.g. current GDP (which is not observed due to publication lags), and X_t is a vector of observable variables at time t . At each time t , the Kalman filter is deployed in two stages. The first is the *prediction* stage: given a previous estimate of Y_{t-1} , predict Y_t . The second is the *correction* stage: as more information about X_t arrives, update the estimate of Y_t .

To be precise, assume that the ground truth is given by the linear equations:

$$Y_t = AY_{t-1} + W_t, \quad X_t = CY_t + V_t,$$

with initial condition $Y_0 \sim N(\mu_{0|0}, P_{0|0})$. Here W, V are independent white noise processes in \mathbb{R}^d and \mathbb{R}^m respectively, with $W_t \sim N(0, \Gamma)$ and $V_t \sim N(0, \Sigma)$, mutually independent at all time points. Note A and Γ are in $\mathbb{R}^{d \times d}$, $C \in \mathbb{R}^{m \times d}$, and $\Sigma \in \mathbb{R}^{m \times m}$. Assume all parameters are known and write $\mathcal{X}_t = (X_1, \dots, X_t)$ to describe observations up to time t .

For the prediction stage, $Y_t | \mathcal{X}_s$, $t \geq s$, is normally distributed, so we can write $Y_t | \mathcal{X}_s \sim N(\mu_{t|s}, P_{t|s})$. Using the dynamics of Y and X , we obtain the prediction equations:

$$\begin{aligned} \mu_{t|t-1} &\equiv E[Y_t | \mathcal{X}_{t-1}] = A\mu_{t-1|t-1}, \\ P_{t|t-1} &\equiv \text{var}(Y_t | \mathcal{X}_{t-1}) = AP_{t-1|t-1}A^\top + \Gamma. \end{aligned}$$

Given new information, the updated mean estimate is

$$\mu_{t|t} \equiv E[Y_t | \mathcal{X}_t] = E[Y_t | X_t, \mathcal{X}_{t-1}] = \mu_{t|t-1} + (P_{t|t-1}C^\top S_t^{-1})(X_t - C\mu_{t|t-1}), \quad (4)$$

while the variance correction equation is given by the discrete-time Riccati equation

$$P_{t|t} \equiv \text{var}(Y_t | X_t, \mathcal{X}_{t-1}) = (I - (P_{t|t-1}C^\top S_t^{-1})C)P_{t|t-1}. \quad (5)$$

This method generalises to the case where the parameters are time-varying.

3.2 Continuous time state-space models

We wish to work with irregular and mixed frequencies. In order to treat timings of observations that are variable, it is natural to embed the discrete-time model in a continuous-time framework. As pointed out in Harvey (1990), p.479, “[a]lthough missing observations can be handled by a discrete time model, irregularly spaced observations cannot. Formulating the model in continuous time provides the solution. Furthermore, even if the observations are at regular intervals, a continuous time model has the attraction of not being tied to the time interval at which the observations happen to be made.” (Also see Bergstrom (1984).) The most natural continuous-time extension of the Kalman state-space model is the Kalman–Bucy filter.³ As in the discrete time setting, assume a hidden process Y (this is the economic variable we are interested in, e.g. current GDP) and observed process X . In this case, assume the ground truth is of the form

$$\begin{aligned} dY_t &= (FY_t + f)dt + \sigma dV_t, \\ dX_t &= (HY_t + h)dt + \tilde{\sigma} dW_t, \end{aligned}$$

where $F \in \mathbb{R}^{d \times d}$, $\sigma \in \mathbb{R}^{d \times p}$, $f \in \mathbb{R}^d$, $H \in \mathbb{R}^{m \times d}$, $h \in \mathbb{R}^m$, $\tilde{\sigma} \in \mathbb{R}^{m \times \tilde{p}}$. Hence, Y is d -dimensional and X is m -dimensional. (We can also allow the coefficients to be deterministic functions of time, with minimal changes.) The processes V and W are Brownian motions and (for notational simplicity) we assume W is independent of V . By computing the Moore–Penrose pseudoinverse $\tilde{\sigma}^\dagger$, and hence replacing X with $\tilde{\sigma}^\dagger X$ (and modifying H and h accordingly), we can assume without loss of generality that $\tilde{\sigma}$ is an identity matrix, for ease of presentation.

The filter, which estimates the current state of the underlying process Y , is then characterised by the following pair of stochastic differential equations

$$d\hat{Y}_t = (F\hat{Y}_t + f)dt + R_t H^\top (dX_t - (H\hat{Y}_t + h)dt), \quad (6)$$

$$\frac{dR_t}{dt} = \sigma\sigma^\top + FR_t + R_t F^\top - R_t H^\top H R_t. \quad (7)$$

Here, $\hat{Y}_t = \mathbb{E}[Y_t | \mathcal{F}_t^X]$ denotes the optimal estimate (in the mean square sense) of the unobserved state Y_t , conditioned on the information available from the observed process X up to time t , that is, $\mathcal{F}_t^X = \sigma(X_s : s \leq t)$. The matrix $R_t \in \mathbb{R}^{d \times d}$ is the conditional covariance of the estimation error

$$R_t = \mathbb{E}[(Y_t - \hat{Y}_t)(Y_t - \hat{Y}_t)^\top | \mathcal{F}_t^X].$$

Note that R_t evolves deterministically according to the Riccati Equation (7), it does not depend on the realisation of the observed process X , but only on the system parameters and time. Once R_t is solved, it can be used in Equation (6) to obtain the filter estimate \hat{Y}_t from the

³For a detailed study of these equations, and derivation of the filter, see for example Bain and Crisan (2008) or Cohen and Elliott (2015, Chapter 22).

observed data. The pair (\hat{Y}_t, R_t) fully characterises the conditional distribution of Y_t given the observations: $Y_t | \mathcal{F}_t^X \sim \mathcal{N}(\hat{Y}_t, R_t)$. In essence, up to changes of notation, the continuous-time mean equation (6) is completely analogous to the discrete-time mean equation (4), and similarly for the variance equations (7) and (5). Unsurprisingly, the discrete-time equations naturally arise as Euler–Maruyama discretizations of the continuous dynamics on a regular grid. However, a key advantage of the continuous-time perspective is that irregular observations can also be considered, leading to different discretisations.

It is worth noting some characteristics of the (discrete or continuous) Kalman filter. First, the various parameters are assumed known – typically in practice these must be learned from data. (This can be done, for example, using the EM algorithm (Dempster et al., 1977).) More significantly, the system is assumed to follow linear dynamics. This can be relaxed using variants such as the Extended Kalman Filter, which assumes the processes are non-linear stochastic dynamic processes (Jazwinski, 1970).

3.3 Paths and signatures

In this section, we introduce terminology and definitions related to paths and signatures. For a more detailed introduction see Chevyrev and Kormilitzin (2025); Fermanian (2021); Lyons et al. (2007).

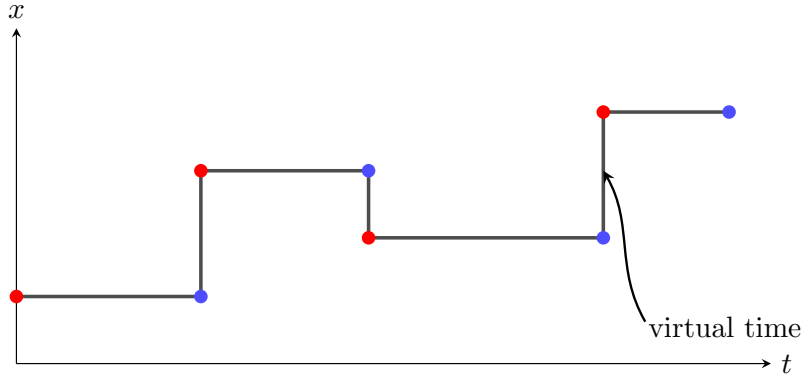
The key insight of the signature method we will propose is that we can treat a wide variety of nowcasting problems, with irregular and mixed frequency observations, by widening our view to consider our observations as ‘paths’ in time and space. By thinking of paths, rather than discretely observed time-series, as our fundamental object, we obtain a unified approach, and open up the use of a variety of approximations, based on the mathematics of paths.

Formally, a path in \mathbb{R}^d is defined as a continuous function $X : [a, b] \rightarrow \mathbb{R}^d$, where each component is a one-dimensional path $X^k : [a, b] \rightarrow \mathbb{R}$, $k \in \{1, \dots, d\}$. For a given sequence of observations, there are a variety of ways we can think of recovering a ‘path’ from these observations. Suppose the j th component is observed at times $\{t_{i,j}\}_{i \in \mathcal{I}_j}$, for some countable index \mathcal{I}_j . A particularly elegant path can be constructed by first considering the map $t \mapsto (t, \{X^j_{[t]_j}\}_j)$, where $[t]_j = \max_i \{t_{i,j} : t_{i,j} \leq t\}$ gives the time of the most recent observation of the component X^j . This function is not continuous, but has the simple interpretation that it represents the ‘most recent observations’ (or equivalently, is the result of forward filling⁴ our observations). We can then extend this function by connecting the jumps in observations, to obtain the ‘rectilinear path interpolation’. This is illustrated in Figure 1.

This construction of a path is somewhat artificial, but demonstrates that any sequence of discrete observations can be represented by a path, without changing the flow of information through time. Importantly, this allows us to represent all observation sequences (at mixed frequencies and with irregular observations) in the same space, as all of them can be considered to be paths. In particular, we do not have to assume that our observations should be sam-

⁴As the goal of this construction is the path, the choice of forward filling does not imply that we believe unobserved values are well approximated by constants, but simply acts as a representation of our observation values.

Figure 1: Rectilinear interpolation. Here real observations (red) are first forward filled, resulting in a piecewise constant function. In order to obtain a continuous path (without changing the flow of information), the values immediately before (blue) and after (red) a new observation are connected vertically using ‘virtual time’. The resulting rectilinear interpolated path has a longer length than the original observations, but describes the available information precisely in a consistent manner for all sampling regimes.



pled at high-frequency, as the ‘observation path’ is a well-defined object even with infrequent observations⁵.

The difficulty of working with paths is that it is not immediately apparent how to use these as statistical objects. The path signature is a mathematical object that describes time-series-like data and is closely related to the theory of rough paths (see Friz and Hairer (2020)). It is a property of continuous paths and has been shown to be an effective description of intertemporal information in prediction tasks – for example in Chinese handwriting recognition (Graham, 2013), sepsis detection (Morrill et al., 2020), malware detection (Cochrane et al., 2021), and time series generation (Ni et al., 2021). Intuitively, the signature allows us to describe ‘polynomial’ functions of paths, in a mathematically rigorous way.

The signature is defined through an iterative construction. Let

$$S^1(X^k)_{a,t} \equiv \int_a^t dX_s^k = X_t^k - X_a^k, \quad k \in \{1, \dots, d\},$$

and let the double iterated integral be

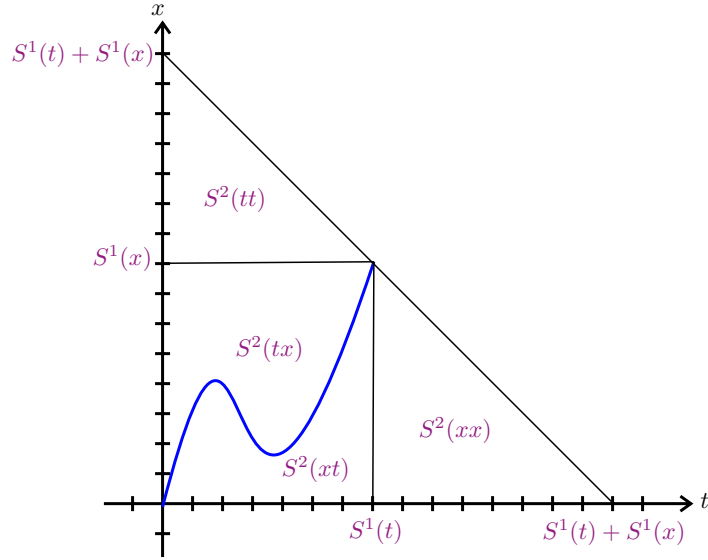
$$S^2(X^k X^l)_{a,t} \equiv \int_a^t S^1(X^k)_{a,s} dX_s^l = \int_a^t \int_a^s dX_r^k dX_s^l, \quad k, l \in \{1, \dots, d\}.$$

More generally define the n-fold iterated integral by

$$S^n(X^{k_1} X^{k_2} \dots X^{k_{n-1}} X^{k_n})_{a,t} \equiv \int_a^t S^{n-1}(X^{k_1} X^{k_2} \dots X^{k_{n-1}})_{a,s} dX_s^{k_n}, \quad k_i \in \{1, \dots, d\}.$$

⁵One might ask whether there is a sense that, when observations become increasingly frequent, the path should converge to a continuous observation path. This is indeed the case, as we discuss in Appendix F. However, in many problems observation frequencies are not within our control, and so we will think of the path constructed from discrete observations as the primary object, rather than as an approximation of an unobtainable ideal path.

Figure 2: Illustration of the first two levels of the signature for a two-dimensional path (with variables t and x).



The superscript in $S^2(X^k X^l)_{a,t}$ denotes the number of iterated integrals, the subscript indicates the limits of the outermost integral, and the terms inside the brackets give the order of integration, starting with the innermost integral. The number of iterated integrals taken is the “level” of the signature. The signature of the path is the ordered infinite collection of all such iterated integrals

$$S(X)_{a,b} \equiv \left(1, S^1(X^1)_{a,b}, \dots, S^1(X^d)_{a,b}, S^2(X^1 X^1)_{a,b}, S^2(X^1 X^2)_{a,b}, \dots\right).$$

The path signature captures geometric information. The first level signature terms give the change/increment in each dimension between the start and end of the path. The second level terms are linked to areas bounded by the path. Figure 2 offers a visual representation of the intervals and areas captured by the first and second level signature terms for a two-dimensional path $X : [0, T] \rightarrow \mathbb{R}^2$ starting at the origin, with the dimensions denoted by x and t . Notice that $S^1(x)_{0,s} = x_s - 0 = x_s$ and $S^1(t)_{0,s} = t_s - 0 = t_s$, i.e. the increments in each dimension. For second level terms, we have $S^2(x, t)_{0,s} = \int_0^s S^1(x)_{0,u} dt_u = \int_0^s x_u dt_u$, $S^2(x, x)_{0,s} = \int_0^s S^1(x)_{0,u} dx_u = \int_0^s x_u dx_u = 1/2x_s^2$, and similarly $S^2(t, x)_{0,s} = \int_0^s t_u dx_u$ and $S^2(t, t)_{0,s} = 1/2t_s^2$. In particular, cross terms, $S^2(X^i X^j)_{a,b}$, $i \neq j$, register how some dimensions tend to change before others and is related to the Lévy area for the path.⁶ These and higher signature levels thus serve as a “geometric footprint” for the path.

Considering the signature as a class of approximating functions, there is a (Stone–Weierstrass)

⁶For a two-dimensional path, the Lévy area A is given by

$$A = \frac{1}{2} (S^2(X^1 X^2)_{a,b} - S^2(X^2 X^1)_{a,b}).$$

The Lévy area encodes the order of events, where a positive value of A indicates X^1 is typically followed by X^2 . See Yang et al. (2017) for further discussion.

theorem that gives universality of this approximation class (Levin et al., 2013). That is, any continuous function on paths can be approximated arbitrarily well through a linear combination of signature terms.⁷ Intuitively, as mentioned above, linear functions of signatures behave like “polynomial functions of paths”. Because of this, all estimation procedures involving learning from paths can be approximated (arbitrarily well) using a linear function of the signature.

As signature terms are iterated path integrals, they inherit the invariance properties of path integrals. The terms are invariant to translation of the path and to any monotonic increasing reparameterisation in time.

The mathematical theory underpinning signature methods is well-developed, with several key results supporting both theoretical analysis and practical computation. For example, Chen’s identity (Chen, 1954) provides a way to compute the signature of a concatenated path⁸ as an algebraic product of individual path segments. This identity allows for recursive or piecewise computation of signatures, making it especially useful for when the data arrives in batches, as long paths can be processed incrementally rather than recomputed from scratch. As a result, Chen’s identity plays a vital role in the efficient and scalable computation of signatures.

3.4 Practical signature computation

In the previous section, we explained that the signature is a natural object for describing paths in general and time-series data in particular. However, when working with real data, we only observe variables at discrete intervals, rather than continuous paths. As a result, we need to interpret new data releases as coming from some underlying continuous time process and exploit connections to model the target variable. Using signatures as features is a natural way to make sense of data released irregularly in continuous time and sidesteps the mixed frequency and missingness challenges covered in Section 2.

There are many choices we can make to approximate the signature, and different methods are suitable depending on the points in time when we want to make a prediction. As signatures describe continuous paths, but data are typically discrete, we must interpolate the observations, to form a path, before computing the signature. The choice of interpolation can matter, and has been explored (Morrill et al., 2022), but in general the signature should not be greatly affected by the frequency of sampling. Smooth cubic splines can be used when only a single prediction is made, as this interpolation is not causal. Rectilinear interpolation (as discussed above) is more appropriate for data measured at different times and frequencies when a prediction may be needed at any point. In nowcasting, we have an online/causal problem (that is, we only want predictions to be made based on available information) where we wish to make inferences at given points: in this case, the interpolation method employed should be either continuously online or discretely online (see Morrill et al. (2022) for more details). In practice, we can use forward filling (discretely online) and rectilinear interpolation (continuously online) in this setting.

The number of signature terms at each level is dependent on the dimension of the path:

⁷For further information on approximation results, see Appendix F.

⁸A path formed by joining two or more path segments end-to-end.

this means that if the number of explanatory variables is fixed, the number of signatures at each level is fixed too. In practice, the iterated integrals that define signatures can be efficiently computed with software packages such as `iisignature` (Reizenstein and Graham, 2020) and `esig` in Python.

It is important to note that the number of terms increases exponentially with the level of the signature, that is, for a d -dimensional path, the signature truncated at the k th level, contains $\sum_k d^k$ terms. So, while signatures can universally approximate any path objects, they do so with an exponentially increasing number of terms, and including all of these would increase model complexity and could result in over-parameterisation.

However, an important result in rough paths limits the extent to which the exponentially increasing number of levels is a problem: the magnitude of signature terms decays factorially with increasing levels (Lyons et al., 2007). If we take $X : [0, T] \rightarrow \mathbb{R}^d$ to be a path with finite one-variation (total variation), i.e.

$$\|X\|_{1,[0,T]} \equiv \sup_{P \in \mathcal{P}} \sum_{i=0}^{n_P-1} |X_{i+1} - X_i| < \infty,$$

where \mathcal{P} is the set of all partitions of $[0, T]$ and n_P is the number of points in partition P , then, for each level $k \geq 1$,

$$S^k(X \dots X)_{[0,T]} = \int_0^T \dots \int_0^{t_1} dX_{t_0} \dots dX_{t_{k-1}} \leq \frac{\|X\|_{1,[0,T]}^k}{k!}. \quad (8)$$

Therefore, as the level of signature terms increases, the magnitude of the terms decreases factorially – which is faster than exponentially – and we still obtain a good approximation to the signature by truncating it at a sufficiently high level.

There are two different ways to incorporate information into nowcasting models, and trained prediction models in general: *expanding window*, where new information is appended to existing data, or *rolling window*, in which data older than a certain lookback period is discarded from the model. When using an expanding window, certain terms in the signature may be increasing. For example, the first level signatures terms are just the differences/increments between the start and the end of the path, and therefore the signatures corresponding to time can increase as more observations become available.

Due to the invariance to reparameterisation property of signatures, it is common to manually add time as one of the input variables if the rate at which things occur is relevant (as is typical in prediction problems). Adding time as one of the variables is referred to as *time-augmentation*. This also ensures that signatures are unique (Hambly and Lyons, 2010). In the methods we consider, we will always make use of the time-augmented path. Other information that can boost performance, especially in contexts where data are not missing at random, include the time since the last observation or counts of the number of observed measurements (Morrill et al., 2022).

3.5 The signature as a source of features in prediction

In this section, we briefly review the use of signatures as features and highlight some variations of “signature methods” in other applications.

One very useful property of truncated signatures is that if two paths are “close” (under the 1–variation norm), then the truncated signatures of these paths will also be close (Giusti and Lee, 2020). Combined with the universal approximation property (by the Stone–Weierstrass Theorem (Levin et al., 2013)), signatures therefore should be good candidates to generate features for prediction or classification tasks. Further, because linear combinations of signatures can effectively capture non-linear relationships, even linear regression via ordinary least squares is theoretically sufficient to model non-linear problems.

Regression on features from signatures has been used in high-frequency financial time series (Lyons et al., 2014; Levin et al., 2013) and in freight transportation price forecasting, where it provided an annualised saving of \$50m for Amazon (Gu et al., 2024). Fermanian (2020) looked at functional linear regression where information on predictors over time is available; this is similar to the setting of economic nowcasting. Fermanian (2020) showed that signature regression is competitive with traditional functional regression methods such as functional principal components and B-splines.

The truncation level can be chosen in different ways. One of the simplest is hyper-parameter search (Morrill et al., 2021b) but others have taken more systematic approaches. For example, Fermanian (2020) assumes that the true model is linear in some truncated signature space: that is the model can be replicated with some m^* . An estimator for the truncation level \hat{m} is designed to minimise the sum of the mean square error of the model and a penalty based on model complexity. This estimator is used with Ridge regression for their functional regression model. Bleistein et al. (2023) show that, using LASSO for regularisation, the truncation error decays exponentially fast with the truncation level.

Note that there are other choices to be made in deriving features from signatures, some of which might be called “model tuning”, that we do not fix *a priori*. Some attempts have been made to systematically categorise the types of operations and model choices that can be made. For example, Morrill et al. (2021a) splits these choices into what they call “modifications” with four primary groups: augmentations, windows, transforms, and rescalings. We forgo further discussion of these techniques, in the interest of focusing on the core simplicity of the method.

3.6 Signatures generalise linear Kalman filters

In this section we show that the Kalman–Bucy filter of Equation (6) is equivalent to a linear regression problem on the signature space. In other words, we can express \hat{Y} as a linear combination of the iterated integrals of the time-augmented observation process (t, X_t) . Though this can be derived more abstractly from the general universal properties of the signature previously mentioned, we provide a formal proof.

The equivalence result we prove holds in any dimension of observation and filter processes. Therefore, it includes the full range of (continuous time) vector autoregressive and linear state-

space models. This suggests that linear regression on signatures has the benefit of avoiding many of the modelling restrictions needed in order to apply filtering methods in situations that are of great practical relevance.

Theorem 1. *The continuous time Kalman–Bucy filter \hat{Y} (including the case with deterministic time-varying parameters), as described by Equation (6), can be written as a linear function of the initial estimate \hat{Y}_0 and the signature of the augmented observation process (t, X_t) . In particular, this representation uses only the signature terms where the observation X appears once in the iterated integral.*

Proof. With the natural time-varying change to the notation set out in Section 3.2, write

$$\begin{aligned} A_t &\equiv F_t - R_t H_t^\top H_t, \\ \xi_t &\equiv \int_0^t (f_s - R_s H_s^\top h_s) ds + \int_0^t R_s H_s^\top dX_s, \end{aligned} \quad (9)$$

which gives us the simplified expression for the filter

$$d\hat{Y}_t = A_t \hat{Y}_t dt + d\xi_t. \quad (10)$$

Denote the iterated integrals of A and ξ by

$$\begin{aligned} \mathbb{A}_t^n &= \int_0^t \int_0^{t_1} \cdots \int_0^{t_{n-1}} (A_{t_1} A_{t_2} \cdots A_{t_n}) dt_n \cdots dt_1, \\ \Xi_t^n &= \int_0^t \int_0^{t_1} \cdots \int_0^{t_{n-1}} (A_{t_1} A_{t_2} \cdots A_{t_n} \xi_{t_n}) dt_n \cdots dt_1, \end{aligned}$$

with the conventions $\mathbb{A}^0 = \mathbb{I}_d$ (the identity matrix) and $\Xi_t^0 = \xi_t$. Observe that these are both formally solutions of the recurrence relation $Q_t^n = \int_0^t A_s Q_s^{n-1} ds$ with different values for Q^0 (and in different dimensions). We note that the n th iterated integral is super-polynomially small (that is, it satisfies Equation (8)), and in particular the infinite sums $\sum_{n \geq 0} \mathbb{A}_t^n$ and $\sum_{n \geq 0} \Xi_t^n$ are both well defined.

Writing \hat{Y} in integral form, we have

$$\hat{Y}_t = \hat{Y}_0 + \int_0^t A_s \hat{Y}_s ds + \xi_t.$$

This integral equation has a unique solution, which can be represented as the series

$$\hat{Y}_t = \sum_{n \geq 0} (\mathbb{A}_t^n \hat{Y}_0 + \Xi_t^n).$$

Given the recurrence relation mentioned above, we can see that this is a solution to the integral equation. This shows that \hat{Y}_t is a (linear) function of its initial value \hat{Y}_0 and the iterated integral processes \mathbb{A}^n and Ξ^n . This expansion is very closely related to the Picard series approximation of the stochastic differential equation defining \hat{Y} (Equation (6)).

It remains to show that \mathbb{A}^n and Ξ^n can be expressed in terms of the (joint) signature of

the time-augmented path (t, X_t) . As A is a continuous deterministic function of time, we know that (over any finite time horizon) it can be approximated arbitrarily well by a polynomial (by the Stone–Weierstrass theorem). As the signature of time is simply the sequence $\mathbb{S}(t) = (1, t, t^2/2, \dots, t^n/n!, \dots)$, we see that A can be written as a (matrix-valued) linear function of the signature of t .

The process ξ in Equation (9) is slightly more delicate, as it depends on both time and the observations X . The first term $\int_0^t (f_s - R_s H_s^\top h_s) ds$ is deterministic, so again has a polynomial expansion in terms of the signature of t . Considering the second term $\int_0^t R_s H_s^\top dX_s$, we see that if H is continuous⁹, $R_s H_s^\top$ has an expansion in terms of the signature of time, so $\int_0^t R_s H_s^\top dX_s$ has an expansion in terms of the signature of (t, X_t) , with the special form where the only integral with respect to X is the outermost one.

As both A and ξ have expansions in terms of the signatures of t and (t, X) respectively, it follows that their iterated integrals \mathbb{A} and Ξ also have expansions of this type. For our purposes the explicit values of this expansion are not of particular interest (and do not have a simple algebraic form), but the definition of \mathbb{A}^n immediately shows that if A can be written as a polynomial in time, then so can \mathbb{A}^n for each n . Similarly for Ξ^n , but now this will involve iterated integrals with a single X integral included. ■

The absence of iterated integrals with more than one X integral in the theorem above is equivalent to the linear dependence of the filter \hat{Y} on the observations X . We refer to the iterated integrals with only a single X integral as “linear” signature terms.

The construction above shows that we can expand \hat{Y} in terms of the initial estimate \hat{Y}_0 . The next lemma shows that we have great flexibility when constructing our signature expansion for the filter, as we can use the signature over any sufficiently large horizon in our representation of the filter.

Lemma 1. *For a continuous path \hat{Y} , and any time $t \in [0, T]$, the value of \hat{Y}_0 can be expressed as a linear function of \hat{Y}_t and the linear signature terms of (t, \hat{Y}) . Consequently, we can express the Kalman–Bucy filter \hat{Y}_t as a linear function of \hat{Y}_s and the linear signature of X on $[s', T]$, for any $s' \leq s < t$.*

Proof. We first focus on the expression for \hat{Y}_0 . The iterated integrals of time give polynomials (of the form $t^n/n!$). By using the inner products

$$\begin{aligned} \langle \hat{Y}, t^n/n! \rangle_{L^2} &= \frac{1}{n!} \int_0^T \hat{Y}_s s^n ds \\ &= \hat{Y}_0 \frac{T^n}{n!} + \frac{1}{n!} \int_0^T \left(\int_0^s d\hat{Y}_u \right) s^n ds \end{aligned}$$

⁹If H is not continuous, then we need to use the fact that polynomials in time are dense in the $L^2([0, t])$ space, which is the appropriate space to consider given we have an outer integral with respect to the process X . In this case we will still have a polynomial approximation $p_n(s) \approx R_s H_s^\top$, such that the integral $\int_0^t p_n(s) dX_s \rightarrow \int_0^t R_s H_s^\top dX_s$ converges in a mean-square sense as $n \rightarrow \infty$.

and similarly $\langle t^m/m!, t^n/n! \rangle$. A simple application of integration by parts shows that the final integral term of the above equation can be expressed as the sum of two signature terms, of the form $S^n(\hat{y}t \cdots t)$ and $S^n(t \cdots t\hat{y})$.

Suppose we compute a regression expansion of Y_t in terms of $\{t^m/m!\}_{m \leq M}$. As \hat{Y} is a continuous path, and the polynomials are dense in the L^2 space on $[0, T]$, this (theoretical) expansion perfectly approximates Y_t as we take $M \rightarrow \infty$. It follows that \hat{Y}_t can be evaluated by evaluating a linear function of the signature terms and \hat{Y}_0 . Rearrangement gives the desired expression for \hat{Y}_0 in terms of \hat{Y}_t .

As we can write \hat{Y}_0 in terms of the signature, we now focus on the representation of \hat{Y}_t in terms of \hat{Y}_s and the signature of X on $[s', T]$. By translation, we can assume $s' = 0$. We have seen that \hat{Y}_0 can be expressed in terms of \hat{Y}_s and the linear signature of Y . From Theorem 1, we know that \hat{Y} can be expressed as a linear function of \hat{Y}_0 and the linear signature of X . Therefore, by a direct calculation, the linear signature terms of \hat{Y} can also be expressed as a linear function of \hat{Y}_s and the linear signature of X , as required. \blacksquare

We conclude with an example where we explicitly compute the optimal filter in terms of the signature.

Example 1. Consider the situation where $d = p = m = 1$, $f = h = 0$, $F = -1$, $H = 1$ and $\sigma = \sqrt{3}$. Then our filter equations simplify to

$$\begin{aligned} d\hat{Y}_t &= -\hat{Y}_t dt + R_t(dX_t - \hat{Y}_t dt), \\ \frac{dR_t}{dt} &= 3 - 2R_t - R_t^2. \end{aligned}$$

For simplicity, assume the initial variance is at the steady state $R_0 = R_t = 1$, so we have

$$d\hat{Y}_t = -2\hat{Y}_t dt + dX_t,$$

which can be solved as

$$\hat{Y}_t = e^{-2t}\hat{Y}_0 + \int_0^t e^{-2(t-s)} dX_s.$$

Assuming $X_0 = 0$, the signature expansion of \hat{Y} can also be computed, as was done for Equation (10), with the identity $A_t = -2$ and $\xi_t = X_t$, to give¹⁰

$$\begin{aligned} \mathbb{A}_t^n &= (-2)^n \frac{t^n}{n!} = (-2)^n S^n(t \cdots t) \\ \Xi_t^n &= (-2)^n S^{n+1}(xtt \cdots t), \end{aligned}$$

¹⁰Here we write $S^n(\cdots)$ for the n -fold iterated integral with respect to the sequence indicated (which must be of length n , with the innermost integral listed first); i.e. $S^3(xtt) = \int_0^t \int_0^{t_1} \int_0^{t_2} 1 dX_{t_3} dt_2 dt_1$. Note that in this example all signature terms are taken over the interval $[0, t]$, so we drop the subscript on signatures for convenience.

and hence Theorem 1 yields

$$\begin{aligned}
\hat{Y}_t &= \sum_n \left(\mathbb{A}_t^n \hat{Y}_0 + \Xi_t^n \right) \\
&= \hat{Y}_0 + \sum_{n \geq 1} \left([(-2)^n \hat{Y}_0] S^n(t \cdots t) + [(-2)^{n-1}] S^n(xtt \cdots t) \right) \\
&= \hat{Y}_0 \left(1 - 2t + 2t^2 - \frac{8}{6}t^3 + \frac{16}{24}t^4 + \dots \right) \\
&\quad + X_t - 2 \int_0^t X_s ds + 4 \int_0^t \int_0^{t_1} X_s ds dt_1 \\
&\quad - 8 \int_0^t \int_0^{t_1} \int_0^{t_2} X_s ds dt_1 dt_2 + \dots
\end{aligned}$$

In particular, if t is small, the first few terms of this series provide a good approximation for the value of \hat{Y}_t , in terms of a linear function of the signature. Note that $\hat{Y}_t \approx \hat{Y}_0 - 2\hat{Y}_0 t + X_t$, the single-step Euler–Maruyama approximation Kloeden and Platen (1992) of Equation (6), appears as the first terms in this expansion.

The simple structure we obtain here is due to the assumptions we have made on our state-space model (in particular, the absence of signature terms of the form $S^n(t \cdots txt \cdots t)$ is due to the assumption the variance is in its steady state).

The key advantage of this approach, even while restricting our attention to the Kalman–Bucy state-space model, is that we now have an expansion which is valid¹¹ for all t . This simplifies dramatically the problem of working with data at mixed frequencies, as we can evaluate the filter state at any t , in terms of the corresponding signature terms, rather than having to compute (as is done, for example, in a MIDAS model) a version of the filter that depends on the timing of observations.

A further advantage of signature methods is that they allow us to easily incorporate non-linearity into our state-space models. For example, if our observations X were replaced in the Kalman–Bucy setting by $\bar{X} = \exp(X)$. Then, by Itô’s chain rule, we know that

$$d\bar{X}_t = \bar{X}_t dX_t + \frac{1}{2} \bar{X}_t dt \iff dX_t = \frac{1}{\bar{X}_t} d\bar{X}_t - \frac{1}{2} dt.$$

Substituting into Equation (6), we see that the Kalman–Bucy filter can be written in terms of the modified observation process \bar{X} , and by very similar arguments to before, this would have an expression in terms of the signature, but with terms involving multiple integrals with respect to \bar{X} .

This suggests that using the signature expansion is robust to the specification of the observation time series. That is, *the usual issues around the choice of transformations (whether to use a series, its logarithm, differences, etc...) are less significant when using the signature method, as they are absorbed into the signature expansion.* The price that we pay to capture

¹¹In practice, as with polynomial approximations of the exponential function, the number of terms needed for large t can increase rapidly, along with their coefficients, leading to numerical instability. For this reason, the performance of the approximation is likely to degrade as the time between official releases (where the underlying value Y is observed) increases.

these non-linear relationships is that the expansion contains multiple integrals with respect to \bar{X} , so we lose the ability to write the filter with only the “linear” signature terms and hence all signature terms should be retained in model fitting.

Finally, in Appendix F, we show that regression on signatures retains the consistency properties we would expect from ordinary least squares. In particular, we show that under stationary-ergodic and autocovariance assumptions about the underlying timeseries that we compute signatures from, the parameters obtained from regression on signatures are consistent.

In summary, we have shown that signatures generalise a wide range of nowcasting methods and their variants in any number of dimensions and even with non-linearities, and that regression on signatures has theoretical properties that make it appropriate for use in time series problems.

4 Nowcasting via regression on signatures

In this section we present how to use regression on the signatures of observations for nowcasting.

4.1 Model specification

Let Y_t be the (low-frequency) target variable we wish to nowcast. Let X_t denote the (high-frequency) observed explanatory variables at t . We wish to build an estimate of Y_t based on a previous observation Y_{t-} and observations of $\{X_s\}_{s \in [s', t]}$, where s' is the start of the lookback window. Motivated by the approximation of the Kalman filter in terms of signatures, we suppose that

$$Y_t = \sum_{k=0}^{\infty} (\alpha_k + \beta_k Y_{t-}) \psi_{k,t} + \epsilon_t \quad (11)$$

where

- Y_{t-} is a previous observation of the low frequency target variable that is available at the time of nowcast. This could be the target variable at the beginning of the lookback window over which the signatures are computed, or the most recent available observation;
- $\psi_{k,t}$ is a sequence (for each value of t) of signature terms at level k , including iterated integrals of t and the different components of the observed process X , calculated over the lookback window $[s', t]$ ending at the present
- ϵ_t is a stationary error term with $E[\epsilon_t | Y_{t-}, \{\psi_{k,t}\}_{k=0}^{\infty}] = 0$;
- α_k, β_k are sequences of regression coefficients.

As outlined in Section 3.6, in order to replicate the Kalman filter, we would have $\beta_k = 0$ whenever ψ_k corresponds to a signature term depending on X , and α_k, β_k nonzero only for those signature terms that depend either purely on t , or on a single component of X appearing once in the iterated integral. Both of these restrictions can be relaxed, leading to a richer class of models than can be captured by the (linear) Kalman filter.

In practice, for a fixed finite sample, we must project onto a finite approximation by truncating the terms of the signature at some level $K < \infty$. As discussed in Section 3.5, there are a variety of practices for choosing the signature truncation level K . We follow Morrill et al. (2021b) and select the level through hyper-parameter optimisation. For real-world data, we search over a range of levels (in features and time) up to level 4: this is enough to capture the changes in the area between time-series (see Section 3.3) and higher dimensional equivalents.

Note that if the gaps $t - t_-$ vary significantly over the prediction period, it would make sense to account for this by using a richer class of models, where $t - t_-$ gives another feature for the signature computation. Note also that the signature terms are typically highly multi-collinear. This can be addressed through any standard technique, e.g. using Principal Component Analysis (PCA) to capture the most important information, or using only a smaller number of terms in the expansion.

In the previous section, we explained that the signature is a natural object for describing paths. Moreover, signatures can be efficiently computed with software packages such as `iisignature` (Reizenstein and Graham, 2020) and `esig` in Python. However, when working with a finite sample of data, there are a number of practical issues that must be addressed before computing the signatures. First, we must decide on the observation window used to construct the signature. Second, to approximate the integrals defining the signature, we must use some interpolation method to fill in missing information about the path. Third, we must decide on the truncation level; how many levels of signature terms to retain in the model.

For the observation window, we choose to use a rolling window of fixed length T_w . That is, for each time t , data older than $t - T_w$ (the lookback period) is discarded from the analysis. Just as in non-parametric regression, increasing T_w reduces variance (when the processes are stationary) but introduces bias when there are time-varying parameters. The constructed signature terms also depend on the lookback period length as for example, the first level signature terms are increments between the start and the end of the path. The lookback period length T_w is a hyper-parameter that we choose as part of our hyper-parameter search. Detailed algorithms for regression on signatures can be found in Appendix A.

The path is a continuous time process but data are discrete. The discrete points must be interpolated to compute the signature. In a finite sample, the choice of interpolation can matter, as has been explored (Morrill et al., 2022). Asymptotically, under conditions stated in Appendix F, the approximate signature converges to the true signature. In practice, we consider rectilinear interpolation and forward filling.

4.2 Regularisation

If the number of predictors are large, then even at a maximum truncation level of $K = 4$, the number of signature terms can still be large. Regularisation techniques can be used to reduce over-fitting.

We take the elastic net (Zou and Hastie, 2005), which includes both L1 penalty and L2 penalty terms, and therefore also performs feature selection, which helps to reduce the number

of signature terms used. The optimisation problem being solved is given by

$$\min_{\alpha_k, \beta_k} \left\{ \frac{1}{n} \left\| Y_t - \sum_{k=0}^K (\alpha_k + \beta_k Y_{t-}) \psi_{k,t} \right\|_2^2 + \sum_{k=0}^K \left(\gamma \lambda (\|\alpha_k\|_1 + \|\beta_k\|_1) + \gamma (1 - \lambda) (\|\alpha_k\|_2^2 + \|\beta_k\|_2^2) \right) \right\},$$

where n is the number of time points that data are collected from, γ is the regularisation strength parameter, and $\lambda \in (0, 1)$ is the L1 ratio. The parameters of the elastic net, λ and γ , are found through hyper-parameter optimisation.

Recall that the magnitude of signature terms decreases at a factorial rate with the truncation level, K (see Equation 8). If we introduce regularisation, then the signature terms should be normalised, else we risk eliminating all the higher level terms due to their relatively smaller magnitude. Therefore we standardise the signatures by removing the mean and scaling to unit variance once truncated terms have been obtained (but before using them in regression). For this, we use the `StandardScaler` from `sklearn` (Pedregosa et al., 2011).

4.3 Rolling windows for signatures

In Section 3.6 we saw that we can replicate the Kalman filter with a linear combination of signatures, where the linear signature terms are multiplied by the true value of the hidden process at some past time. In the context of nowcasting, to account for non-stationary behaviour of time series, we can compute signatures of our observations over a rolling or sliding window as discussed in Section 3.4.

Given that we wish to maximise the use of alternative data sources that are more timely than the target variable, our window of information should include at least the last release of the target variable. We therefore assume that the “true” value of the target variable will be available to the model at some point in the window that we compute signatures in, and that we can use that true value as a multiplier. This is denoted by Y_{t-} in Equation (11).

Alternatively, a previous estimate can be used. As explained in Lemma 1, the multiplier can be at any fixed time within the lookback window – but note that different past times will result in different regression coefficients.

4.4 Hyper-parameter selection

Regression on signatures forms a family of approximation functions, with a range of hyper-parameters to optimise over. These include the lookback window length T_w , the truncation level K , elastic net penalty parameters λ and γ .

Hyper-parameters are obtained by running the models over a validation period. The best hyper-parameters are then used to fit the final model on the whole training and validation period, and this calibrated model is used in the test period.

5 Simulation: equivalence to the Kalman filter

In Section 3.6, we proved that the signature method subsumes the linear Kalman filter. We now illustrate this theoretical result in a controlled environment, by comparing the performance of the Kalman filter to regression on signatures (as described in Section 4) on simulated data, and to build intuition before analysing real-data applications. Specifically, we consider four cases: linear observation process with regularly sampled data, linear observation process with irregularly sampled data, non-linear observation process with regularly sampled data, and a non-linear observation process with irregularly sampled data. In each case, we compare the results from the signature method to those from the theoretically optimal Kalman filter (with perfect information of the system). We find that the residuals of the signature method are highly correlated with those from the Kalman filter in all settings except the final case of non-linear process with irregularly sampled data. However, even in this last case, the mean and the variance of the residuals from the signature method remain competitive. This study on simulated data demonstrates that signatures can effectively handle both non-linearity and irregular sampling at essentially no extra effort. In the subsequent sections, the signature method is applied to US GDP data (where there are regular monthly updates on all the predictors) and UK unemployment data (where the data is mixed frequency) – these provide complementary and more challenging case studies for our method.

5.1 Simulation specification

We simulate a 1–dimensional continuous-time state-space model similar to Example 1. The latent state Y_t and its associated linear observation process X_t follows the SDEs

$$\begin{aligned} dY_t &= -Y_t dt + \sqrt{2} dV_t, \\ dX_t &= 10Y_t dt + dW_t. \end{aligned}$$

Throughout this section, we consider two observation regimes. In the first case, we observe X_t directly (where the Kalman filter is optimal). In the second, we observe a non-linear variant, namely a sigmoid transform of X_t

$$\bar{X}_t = g(X_t) = \frac{1}{1 + e^{-X_t}}, \quad \bar{g}(\bar{X}_t) := \frac{dg^{-1}}{d\bar{X}_t} = \frac{1}{\bar{X}_t(1 - \bar{X}_t)}.$$

In this setting, the naive Kalman applied to \bar{X}_t directly is not optimal, the baseline filter is obtained from (6) by replacing dX_t with $\bar{g}(\bar{X}_t) d\bar{X}_t$ (i.e. working with the transformed increments).

In Example 1, by assuming that the variance is in steady state, we derived the coefficients of the optimal filter, \hat{Y} , with respect to its infinite signature expansion. In particular, under the linearity assumptions, the only non-trivial terms in the expansion are signatures that we refer to as “linear” (where only one of the iterated integrals is with respect to the observed data and the rest are time integrals), and further, that the only integral with respect to the data

variables is the innermost one. We adopt these assumptions for the linear observation regime. In contrast, under the non-linear observation regime we can no longer accurately represent the filter using only the innermost linear signatures; instead we must retain all signature terms up to a specified truncation level.

In both cases, we assume the simulated path starts at $Y_0 = 0.1$. Assuming steady-state variance, we can compute $R = H^{-2}(F + \sqrt{F^2 + \sigma^2 H^2})$. The end time, T , is randomly sampled uniformly on $[0.1, 1]$ and the mesh size in time is fixed at $\Delta t = 0.005$.

For the linear observation process, because the dynamics are linear and the true parameter values are known, the ideal (generally infeasible) Kalman filter minimises mean square error. The mean of the filter is given by Equation (6). The discretised optimal filter is then given by

$$\hat{Y}_{t+\Delta t} = \hat{Y}_t + (F - RH^2)\hat{Y}_t\Delta t + RH(X_{t+\Delta t} - X_t).$$

To compare regression on signatures against this optimal but infeasible filter with perfect knowledge of the parameter values, we proceed as detailed in Section 4.

Unlike the Kalman filter, the signature method does not assume the parameter values are known: everything has to be inferred from the data. As the purpose of this exercise is to validate that regression on signatures has the capacity to learn the optimal filter, we utilise a large training set of independent samples to estimate the regression coefficients.¹² We simulate 1000 independent paths (for both X_t and Y_t) of which we take 800 to be in the training set (to calibrate the regression model) and the remaining 200 in the test/evaluation set. For this simulation, we use an expanding window to compute the signatures.

We compute signatures of each observed path (X_t in the linear regime and \bar{X}_t in the non-linear regime). In the linear regime, we truncate at level 6, keeping only the linear signatures of the form $S^n(xtt \dots t)$ as discussed (Example 1). For the non-linear regime we use **all** signatures up to level 3 in the regression, yielding a comparable number of features (15 versus 13).

Overall we conduct four simulation experiments: linear process with regularly sampled data, linear process with irregularly sampled data, non-linear process with regularly sampled data, and a non-linear process with irregularly sampled data. To determine whether the Kalman filter and regression on signatures are similar, we compare the means and variances of their respective residuals.

For the irregularly sampled cases, we randomly drop 80% of the regularly sampled data example above, this is done uniformly at random. The signature-based model is recalibrated using this reduced dataset.

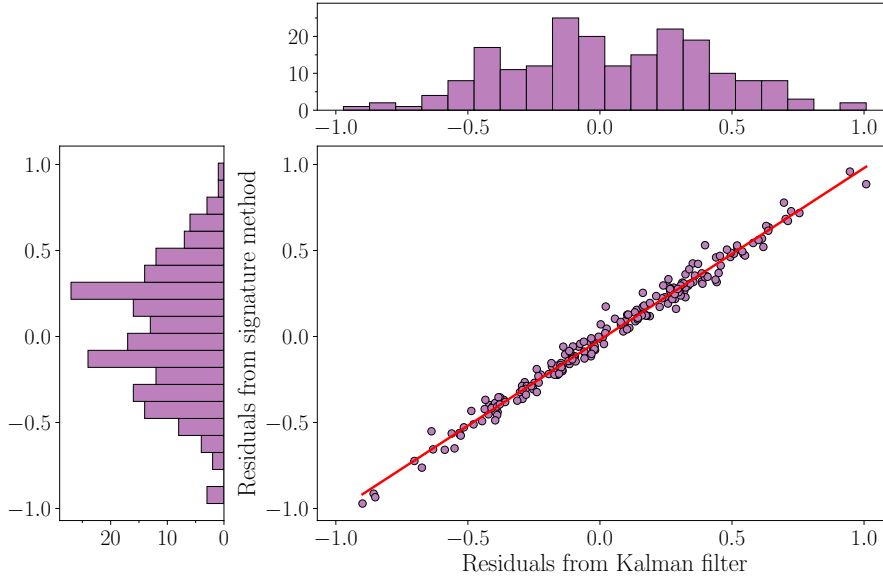
5.2 Simulation results

For the linear case with regular sampling, Figure 3 shows the residuals (difference between target and estimated values) of the Kalman filter and the signature method plotted against one another with a line-of-best-fit. The two approaches perform similarly on the test set. The alignment of the errors of the signature method (where the parameters are fitted from data)

¹²See Appendix F for discussion of consistency in both the independent and dependent sample cases.

against the ideal filter (given full information) is excellent. The means and variances are similar, suggesting that these methods are equivalent means of reaching the same results. The signature method achieves this result without knowledge of the true data generating process.

Figure 3: Residuals of the Kalman filter vs the signature method on regularly sampled data for the linear process. Marginal plots are histograms of residuals. Line-of-best-fit shown in red (gradient 1.00 and y -intercept of -0.02).



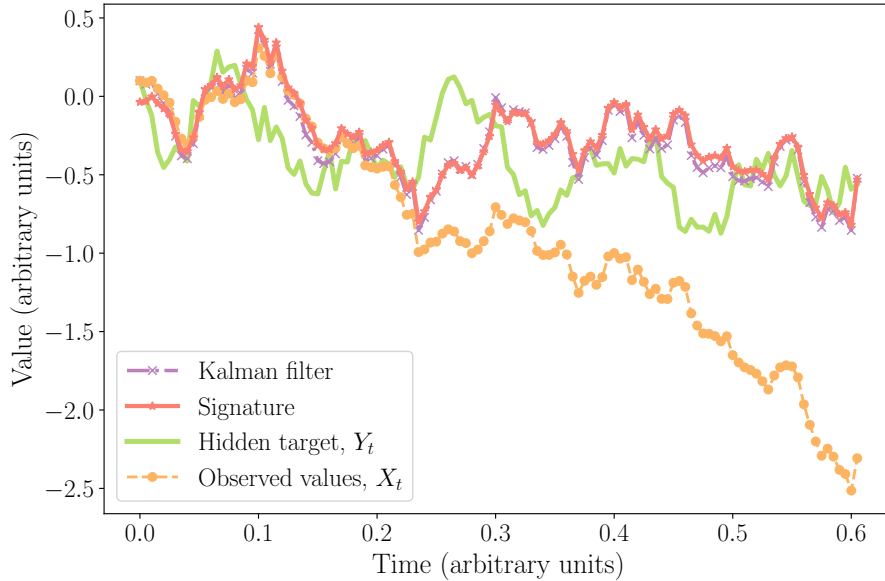
To give a sense of how these models perform in nowcasting contexts, we apply them both recursively on new observations to see how well they infer the path of a hidden target variable. We illustrate the recursively inferred paths on a single example from the test set in Figure 4. The signature method and Kalman filter produce similar trajectories despite the former facing the additional difficulty of inferring unknown parameters from data. Furthermore, both inferred paths are close to the true underlying path, Y_t .

Table 1: Means and variances from simulations: Kalman filter and signature method.

Name	Linear		Non-Linear	
	Regular	Irregular	Regular	Irregular
Kalman residuals (mean)	0.04	0.04	0.02	0.00
Signature residuals (mean)	0.02	0.01	0.00	0.00
Kalman residuals (variance)	0.14	0.15	0.14	0.38
Signature residuals (variance)	0.14	0.14	0.21	0.21

For each of the other three simulation experiments, charts similar to Figures 3 and 4 are presented in Appendix B. Here, we summarise the results in Table 1. The variances of the residuals are extremely similar for the linear cases, and not considerably worse for the non-linear cases. The relationship is harder to learn in the non-linear case, especially with randomly downsampled data. However, despite the observed data having a non-linear relationship with the true, hidden values Y_t , regression on signature terms obtains predictions that closely match

Figure 4: A regularly sampled simulated path (from the test set) with observed values (X_t) along with the true, hidden values that need to be inferred (Y_t).



the theoretical optimum. Regression on signatures can pick out the key information even when the data are more sparse and non-linear.

6 Nowcasting US GDP growth

In this section we apply our proposed methodology to the real-world task of nowcasting US GDP growth. Specifically, we compare our regression on signatures model to the version of the Dynamic Factor Model (DFM) developed by Bok et al. (2018), which was employed by the New York Fed for their staff nowcast prior to the post COVID-19 update by Almuzara et al. (2023).

We refer to the model proposed by Bok et al. (2018) as the “NYFed model”. It provided weekly nowcasts of quarterly US GDP quarter-on-quarter growth using a DFM estimated with 37 monthly macroeconomic variables, released at varying dates over the quarter. In this section we show that nowcasting with signatures (as defined in Section 4) combined with standard dimension reduction methods (e.g. principal components) outperforms the NYFed model. Unfortunately, we cannot use the exact dataset as proposed by Bok et al. (2018) due to data availability constraints (see Section 6.1 for details). Therefore, we compare our model with two benchmarks: (i) the NYFed staff nowcasts published on their website and (ii) the same DFM structure using only publicly available data. This is a standard, well-studied nowcasting problem. We are considering only variables of the same (monthly) frequency, without any missing data. Such a setting does not fully exploit the key strengths of signatures. Nonetheless, our proposed methodology still outperforms both benchmarks, reducing nowcast error by 20%.

6.1 Data

In order to nowcast US GDP, we use 33 of the 37 variables listed in Bok et al. (2018). The four variables we omit (“ISM non-manufacturing: NMI composite index”, “ISM mfg.: Prices index”, “ISM mfg.: PMI composite index”, and “ISM mfg.: Employment index”) are not publicly available. We use University of Michigan: Consumer Sentiment (Curtin, 2008) as a replacement for the ISM series, meaning that we use 34 variables in total. The complete dataset includes a selection of monthly variables that cover housing, income, manufacturing, the labour market, manufacturing activity surveys¹³, trade, and consumption. The indicators are monthly, but due to varying publication lags and frequencies, new information is released each week.

For further details see Appendix D and Table 5.1 of Bok et al. (2018).

6.2 US GDP nowcasting models

Dynamic Factor Model (DFM)

Our baseline model is a DFM based on the NYFed model. The model assumes that the k observed variables, $x_t \in \mathbb{R}^k$, are driven by r unobserved factors $f_t = (f_{1,t}, \dots, f_{r,t})^\top$. In state space form, the model is

$$\begin{aligned}x_t &= \Lambda f_t + e_t, \\f_t &= \sum_{i=1}^p a_i f_{t-i} + v_t, \\e_t &= \sum_{i=1}^q b_i e_{t-i} + w_t,\end{aligned}$$

where $\Lambda \in \mathbb{R}^{k \times r}$ represents the factor loading, $e_t \in \mathbb{R}^k$ is the idiosyncratic noise process in the observations, and $v_t \in \mathbb{R}^r$ and $w_t \in \mathbb{R}^k$ are independent Gaussian random noises. The parameters p and q are the orders of the autoregressive processes of the factors and the idiosyncratic noise process respectively. The NYFed model assumes $p = q = 1$.

In factor models, the factor loadings and factors are not identified without imposing further structure. We follow Bok et al. (2018) and impose a dedicated four-factor structure on the factor loading matrix with the following economic interpretation. The first factor is a “soft” factor, which only includes variables derived from survey data, usually published earlier than official statistic variables. The second and third factors called “real” and “labour”, which refer respectively to activity and labour market variables. The final factor is a global factor, which includes all predictor variables. Details of the variables in each group are listed in Appendix D. These restrictions are sufficient to identify the model parameters.

Bok et al. (2018) extract the factors from the data with the following procedure: At the start, the factors are initialised by finding the principal components of each factor group. Then, there is a two step procedure: first, given the estimated factors, we estimate the loading matrix, dynamic

¹³[Empire State Mfg Survey: General business conditions](#) and [Philly Fed Mfg. business outlook: current activity](#).

coefficients, and variance parameters by least-squares regressions; second, given these estimated parameters, we update the common factors using a Kalman smoother and the Expectation-Maximisation algorithm (see Baum and Petrie (1966); Baum and Eagon (1967); Baum et al. (1970)). Iterations of this EM procedure converge to a local optimum of the likelihood function under standard regularity conditions (Dempster et al., 1977; Wu, 1983).

Regression on signatures with dimension reduction

Here we outline modifications of the signature method to combine it with dimension reduction.

The process is repeated each time new information is received. First, principal component analysis (PCA) is used to find the first principal component of each factor group. We enforce the same dedicated factor structure as in the NYFed dynamic factor model. Then we compute signatures on time and on the time series of factors derived from PCA. Finally, we run a regularised regression of US GDP on the signatures and on the latest available GDP value.¹⁴ Effectively, this means the model learns the change in GDP growth. We label this procedure Signature-PCA.

In fact, given that the signature method is largely agnostic to the data used as inputs, we can also use it as a method to improve existing nowcasts. For example, we can take the mean estimated factors from the NYFed DFM, compute the signature of these “data”, and then use these new signatures to nowcast US GDP growth. This hybrid method allows us to combine forecast methods. We refer to this hybrid method as Signature-DFM.

Model comparison

For each model, when new information arrives (i.e. weekly), we use information from previous quarters to fit the model and then apply the model to nowcast the current quarter’s US GDP growth. We use data from 1st Jan 2000 to 31st December 2015 as the training set, which means that they are always used to fit the regression parameters. From 2016 onward, each week, new data is incorporated into the model (and new factors and principal components are computed) and another nowcast prediction is made for GDP in the current quarter.

The period from 1st January 2016 to 31st December 2017 is used as a validation set to select hyperparameters such as the level of signatures to use and the length of the lookback window. The period 1st January 2018 to 31st December 2019 is then used as a “test set” with fixed hyperparameters, but the regression parameters are still tuned with new data release over the test period. The list of selected hyperparameters can be found in Appendix E.1.

We use root mean squared error (RMSE) as our prediction quality metric.

6.3 Results

We first present NYFed model published results, results from a DFM using only publicly available data, and results from Signature-PCA (signature methods combined with PCA). The

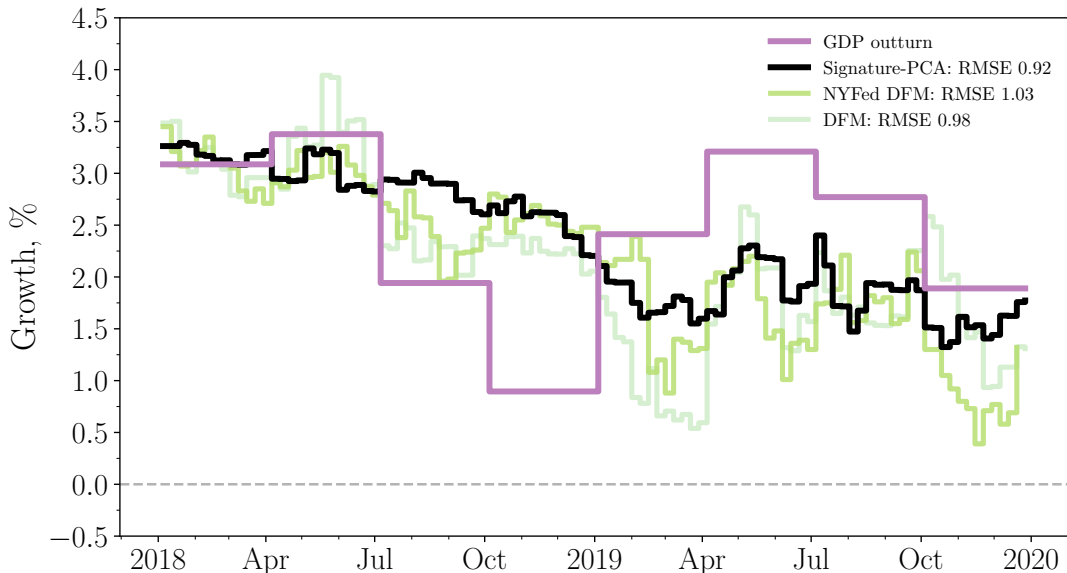
¹⁴Note that this is the latest *published* value – for US GDP, there is a 30-day lag between the end of a quarter and the publication of the data.

Table 2: RMSE for the Signature-PCA, Signature-DFM approaches, as well as our DFM and the NY Fed published values.

Method Period	DFM	NYFed	Signature-PCA	Signature-DFM
Validation	0.85	0.86	0.57	0.46
Test	0.98	1.03	0.92	0.82

headline result is that, in the test period, Signature-PCA outperforms the other approaches. This can be seen in Figure 5.

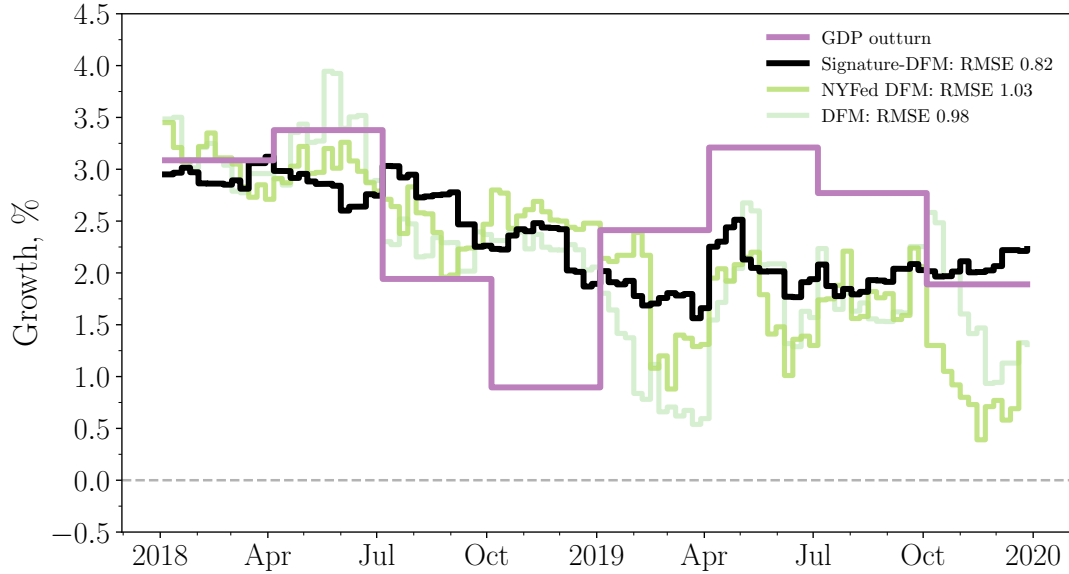
Figure 5: US GDP results for the test period with the signature method is applied to the principal components of the factor groups.



We also fit a hybrid Signature-DFM model. For the validation period, the Signature-DFM approach also strongly outperforms the other methods. For the test period, Figure 6 shows that Signature-DFM is superior to the DFM and to regression on signatures using PCA. Using the DFM model estimates as inputs to the signature approach, produces a noticeable improvement in prediction quality over the DFM alone. This provides evidence that signatures can be incorporated into existing nowcasting models to enhance performance.

The results for all models on validation and test periods are summarised in Table 2. We observe all models giving higher errors in the test period. Using the signature method achieves the lowest root mean squared error, with the filtered factor version of the signature method delivering the best overall performance.

Figure 6: US GDP results for the test period when the signature method is applied to the DFM factors.



7 Nowcasting unemployment: an application of signatures to irregular and mixed frequency data

In this section we demonstrate two more properties of signatures: the ability to handle *mixed frequency* and *irregularly sampled* time series data. As our example, we nowcast the UK’s Office for National Statistics (ONS) monthly unemployment rate (the percentage of those economically active 16- to 64-year-olds in the UK who are unemployed; labour market statistics code I46A). To do this, we use the following high-frequency variables: the weekly benefit claimant count from NOMIS (National Online Manpower Information Service); two monthly Google Trends search series (“unemployment benefit” and “seekers allowance”); and highly experimental ONS weekly time series covering activity, inactivity, employment, and unemployment. The objective is not to create the most accurate nowcast of unemployment (this would be achieved by including many more predictor variables) but to demonstrate the ability of signature methods to tackle irregular and mixed frequency series.

Note that, because we are using high-frequency data, some later updates in the feature series refer to periods *after* the period we are trying to nowcast, and may therefore be less relevant. One way to extract additional information is to treat these post-reference period updates as separate features in the model. This would allow the signature method more flexibility in incorporating their information, compared with the same series pertaining to the reference period of the nowcast. We leave this and other advanced feature engineering approaches to future work.

7.1 Data

Rather than directly target the official monthly unemployment rate, u_t , we follow Anesti et al. (2022) and target the change in unemployment rate relative to the most recently published value, i.e. we transform using first differences. Note that the most recently published official estimate of unemployment can be either u_{t-2} or u_{t-1} depending on the publication lags and when the nowcast is made.

This nowcasting problem involves a complex, time-varying combination of mixed-frequency and irregular data releases. Three of the inputs we use are monthly: the two Google Trends data series and the claimant count variable. The experimental labour market statistics are weekly. Publication dates are irregular with respect to each other; because the number of weeks per month is not an integer, weekly data publication dates move around relative to the end of the month. Publication dates of both prediction variables and target also move around relative to the reference date.

There are also periods when official publications were severely delayed, either by problems at the statistical agency or by external factors such as COVID-19. For example, for June 2020, the official unemployment statistic was published 168 days after the reference date. We include these periods with severe delay in our analysis to demonstrate how well our model copes with unusual circumstances.

We have historical information on reference and publication dates for official releases from 2016 onward. Before 2016, we impute the publication date to be the first Tuesday at least 45 days after the reference date. This is a very accurate rule of thumb for actual publication dates as 45 days is the modal gap for publications from 2016. Since we are using these imputed pre-2016 publication dates simply to demonstrate the performance of signature methods in a hypothetical nowcasting experiment, these imputations do not have any important impact on our results.

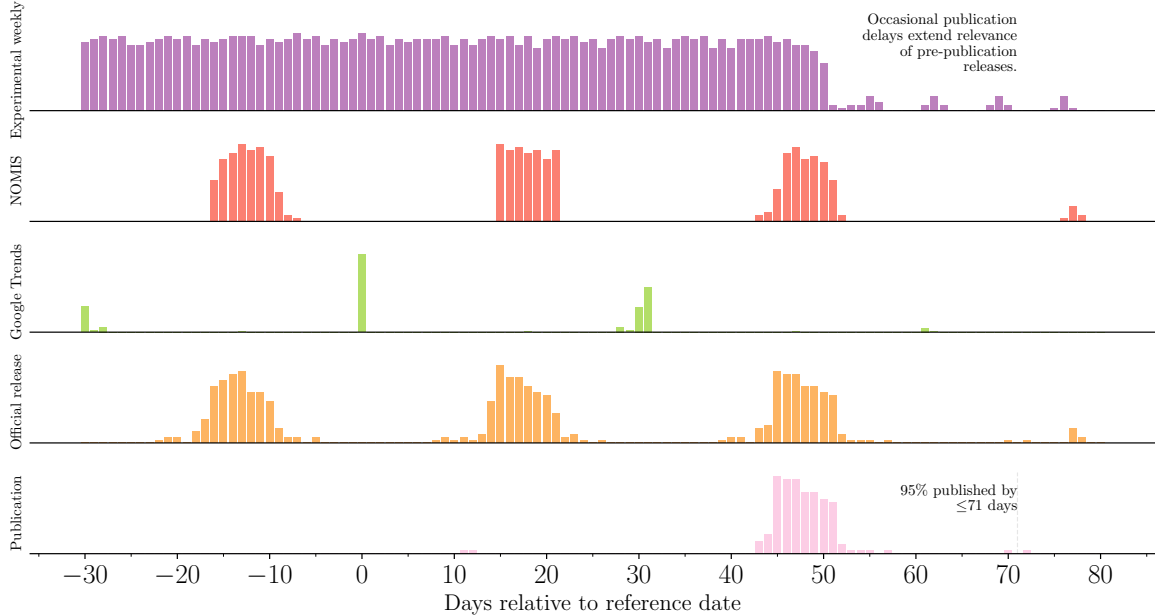
Each nowcast period is defined by a window that begins 30 days prior to the reference date and ends 90 days after it. Within each nowcast period, we produce a new nowcast whenever new information is released. Because of the data irregularities noted earlier, each nowcast period sees data released at slightly different times relative to the reference date. Figure 7 visualises all releases in the data (2008–2023), and how the date of the publication falls relative to the reference date, using a histogram for each information type. The figure shows that, relative to the reference date, information arrives at inconsistent times. Only those releases that are actually used are shown; this is why there are few input series shown after 55 days, when, usually but not always, the unemployment rate has been published.

7.2 Models

We use the regression on signatures nowcasting model outlined in Section 4, with features and data as described above. We use PCA for dimensional reduction, Elastic Net for regularisation, and we include an intercept. We only keep linear signature terms.

One of our baseline models is an auto-regressive model of order 1, AR(1). Although simple,

Figure 7: Each panel shows a histogram of publication dates relative to reference dates with frequencies counted across all nowcasting periods between 2008 and 2023. Only those variables (first four rows) used to inform estimates pre-publication (last row) are shown. Publication dates for both predictor variables and the target variable vary considerably relative to the reference date, except for Google Trends, which is more consistent. In particular, publication dates for experimental weekly data are not in phase with the official publication. See Figure 8 for an example of the timing of information releases in a specific month.



on average and across a wide range of situations, AR(1) models are tough to beat (Carriero et al., 2019).

As the AR(1) only uses lags of the target variable, we also compare the performance of the signature approach to the predictions of a Mixed Data Sampling (MIDAS) model as described in Section 2. We use the L-BFGS-B algorithm to solve the MIDAS model. As with the signature regression model and AR(1), we use a single lag of the target variable in the MIDAS model, as well as 4 lags of each high-frequency (weekly) predictor (4 being roughly the number of weeks in a month).

For all models, we use the period from 2008 to 2020 as both the training and validation period, and 2020 to 2023 as the test period.

7.3 Results

After a hyperparameter search, the selected configuration has $\alpha = 0$, meaning no regularisation and, effectively, OLS – this is not unexpected given the small number of features. A truncation level of 3 is selected and no standardisation of the features is used. The full details of the selected hyperparameters can be found in Appendix E.2.

Figure 8 shows an example nowcast for the reference date of November 2019. This month saw a significant movement in the monthly unemployment rate, which only the signature model

Figure 8: An example nowcast of UK unemployment for the reference date of November 2019. The published value (at the publication date) is shown by a red cross.

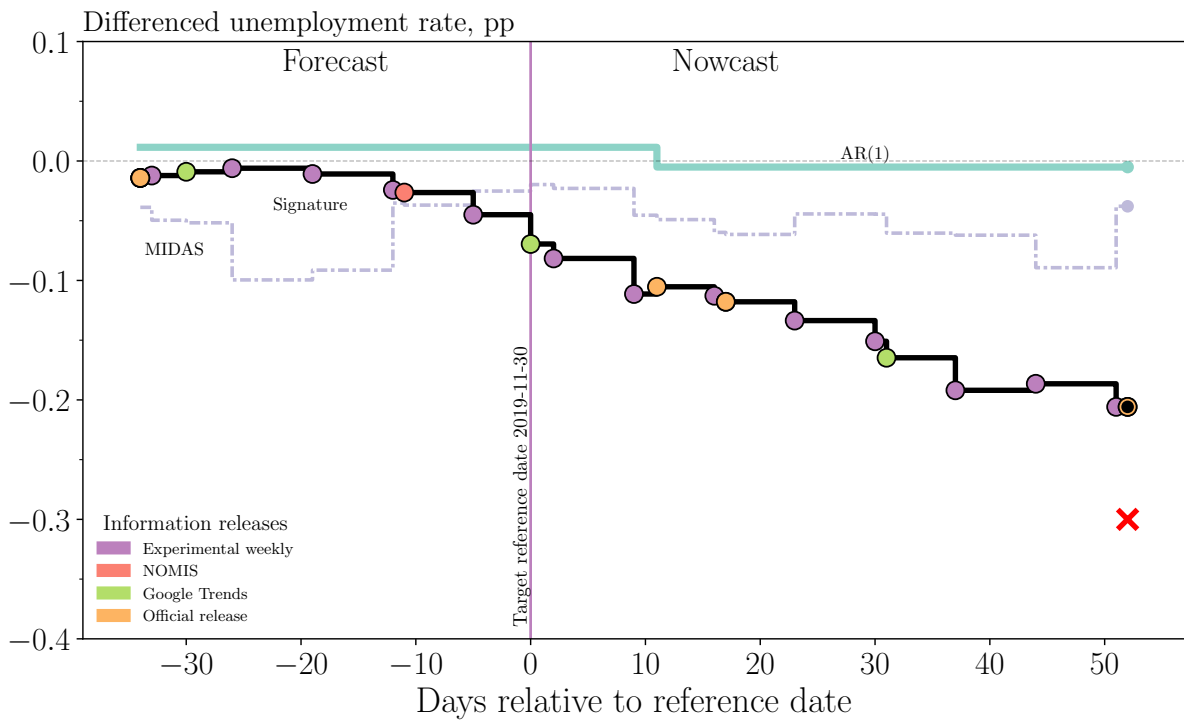
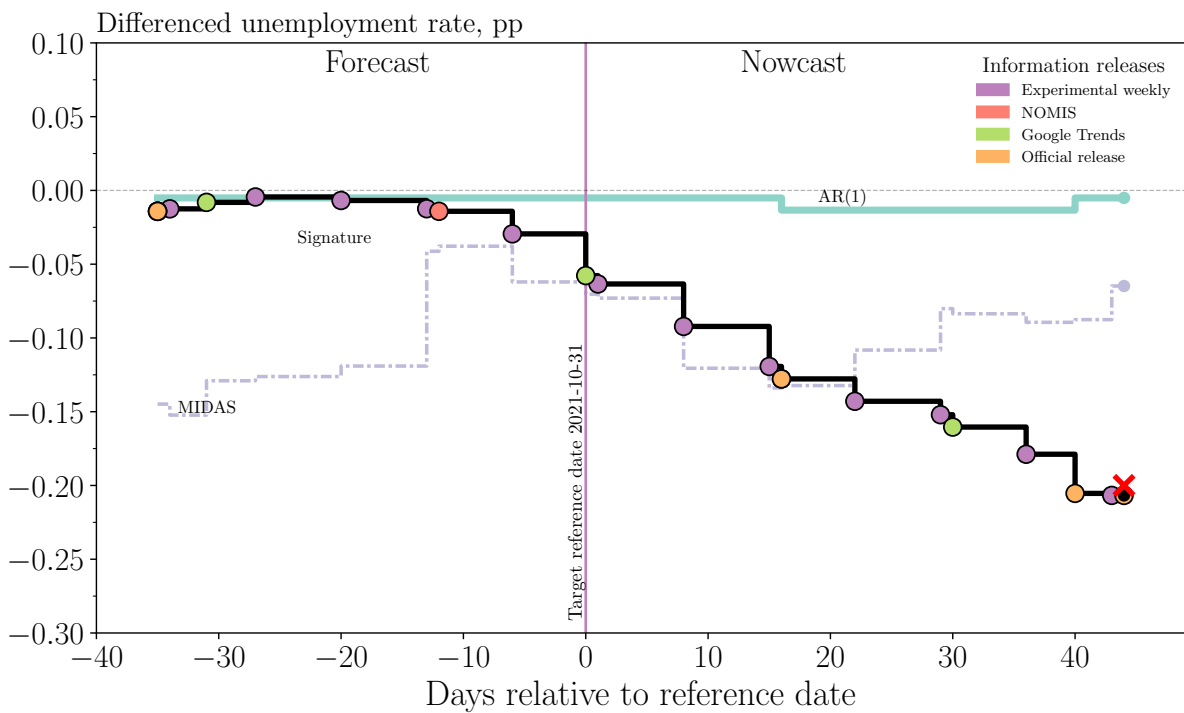


Figure 9: An example nowcast of UK unemployment for the reference date of October 2021, a month after the end of the UK government’s furlough scheme. The published value (at the publication date) is shown by a red cross.



picked up (and even then, undershot.)

Figure 9 shows a nowcast for October 2021. This was a particularly challenging period to

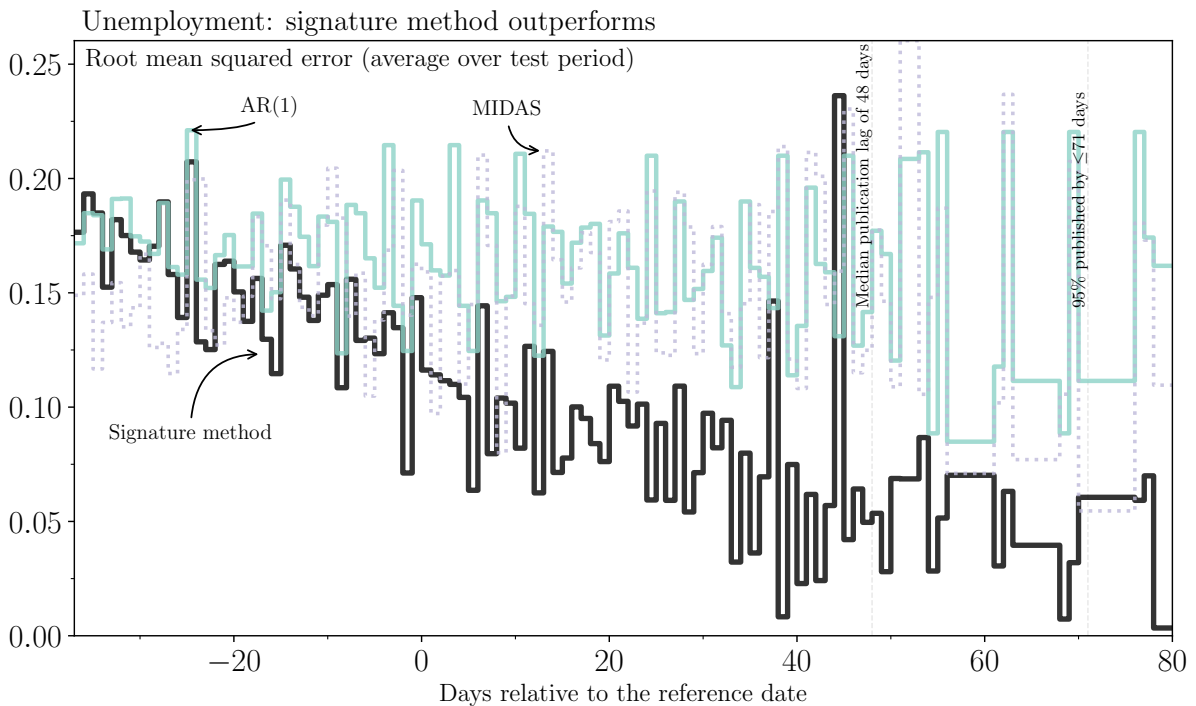
nowcast as it was the tail end of the UK’s COVID-19 pandemic and the furlough scheme (also known as the Coronavirus Job Retention Scheme) had ended the month before.

In both figures, and in general, the AR(1) updates its prediction only as the previous months’ target data become available. The signature method reassesses its prediction with each new information release. Although MIDAS model also updates with the same frequency and uses the same inputs as the signature model, MIDAS fares only slightly better than the AR(1) in these examples.

In Figure 10, we show just how typical it is that the signature outperforms both the AR(1) and the MIDAS model. Figure 10 shows the root mean squared error (RMSE) for all three models averaged over the test period. The signature method consistently outperforms the other two models over relevant publication timeframes, and overall: the average of the RMSEs over the reference periods was 0.169, 0.160, and 0.146 for the AR(1), MIDAS, and signature method respectively.

The variability in the timing of data releases (as shown in Figure 7) is the main reason for the volatility in the average RMSE graph. Note that the publication date moves around relative to the reference date too: it is usually, but not always, on the first Tuesday 45 days after the reference date, with a median publication lag of 48 days. In some cases, the publication was severely delayed, coming out well beyond the usual 48 days. Overall 95% of publication lags are shorter than 72 days, as shown on Figure 10. As far fewer publications occur at lags of 50 days or more, the chart beyond that point is based on averaging over fewer nowcast predictions, leading to a more noisy measure of accuracy.

Figure 10: The average root mean square error of an AR(1) versus a MIDAS model versus the signature method as applied to nowcasting UK unemployment.



There are important conclusions to draw from this exercise. The first is that the signature method is at home with truly difficult time series problems – here, we tackle irregular series, delayed target variable publication, and mixed frequencies. Second, we see that the signature method outperforms the baselines at almost any point during the tracking period. Third, the signature method still performs well in difficult times – even during COVID-19, when employment and economic activity were highly disrupted and the swings in unemployment rate were considerable, the signature method provides a stronger nowcast than the other approaches. This matters enormously for policymaking because it is precisely during disrupted times that decisions really count.

8 Conclusion

The path signature captures geometric properties of sequential data that make for excellent features to use in nowcasting. Signature methods allow for missing data from mixed frequencies or irregular sampling – issues often encountered in nowcasting – by embedding observed data in continuous time. They can also capture non-linear effects and replace the time series modellers’ need to think deeply about data transformations. All of these properties mean signature methods are well-placed to deal with difficult time series problems in general, and nowcasting in particular.

In this paper we demonstrated the application of regression on signatures to nowcasting via what we call the signature method. We introduced the theory of path signatures and illustrated how they are computed, and we showed that regression in the signature space subsumes the linear Kalman filter, which is commonly used in the nowcasting literature. We also validated this through simulations, demonstrating that it is possible to almost replicate the optimal performance of the Kalman filter (when parameters are known) by using regression on signatures (fitting parameters based on data) in simulated experiments, including with irregular data.

We also applied the signature method to some relevant real-world case studies. The first is a well-known empirical exercise: nowcasting US GDP growth. We have shown that incorporating signature features from principal components can offer improvements compared with a dynamic factor model based on Bok et al. (2018). The best results are achieved when we compute signatures on top of the fitted dynamic factors from the baseline DFM, illustrating the value of computing signatures as features even in the presence of informative data series.

The second case study was nowcasting UK unemployment with mixed frequencies and irregularly available data series. We showed that the signature method performs extremely well relative to a benchmark nowcast, that it can give an early indication of the sign of the change in the outturn, and that the performance of the signature holds up even in difficult circumstances – in this case, during the COVID-19 pandemic. Such difficult circumstances are when informing policymakers matters most and therefore we believe the signature method to be an important and useful contribution to nowcasting.

non

A Model Framework

We set out the proposed model framework in two algorithms.

Algorithm 1 gives the procedure to fit a single signature regression model on a set of clean data. The full signature regression method pipeline is presented in Algorithm 2. Note that while this uses hyper-parameter optimisation as part of the pipeline with grid search, other hyper-parameter search strategies could easily be incorporated.

The full list of configuration settings, and a brief explanation of them, may be found in Appendix C.

Algorithm 1: Fit signature regression model

Input:

- cleaned data available (observation & target) in a wide table, pivot format;
- target variable name;
- data parameters, e.g. publication lag in the target variable;
- model parameters associated with signature regression, e.g. the truncation level, lookback window length, whether to use the previous known value of the target etc.; these may be given as lists to perform a hyper-parameter search over.

Process:

1. Define the auxiliary dataframe of available observations.
2. Convert the path information of the observations into truncated signatures over each lookback window.
3. Split signatures into training data and test data. The training data can be a proportion of the data available, or it can be the maximum data available (all timepoints for which the target is available).
4. Fit a (regularised) regression model.

Return: fitted model

B Further simulation results

Here, we provide similar charts to Figures 3 and 4 for the three other simulation cases: irregularly sampled data, data generated by a non-linear process, and irregularly sampled data generated by a non-linear process. The former chart type compares the residuals from a signature regression that has learned parameters from the data versus a Kalman filter that knows the underlying parameter values. For the means and variances of residuals, see Table 1. The latter plot type

Algorithm 2: Signature regression framework

Input:

- cleaned data available (observation & target) in a wide table, pivot format;
- target variable name;
- data parameters, e.g. publication lag in the target variable;
- model parameters associated with signature regression, e.g. the truncation level, lookback window length, whether to use the previous known value of the target etc.; these may be given as lists to perform a hyper-parameter search over.

Impute missing values in the dataset by specified method (defaults to forward fill for all values except those at the beginning, which are filled by backward fill).

for *each set of hyperparameters/configurations* **do**

for *each time over the hyperparameter optimisation period (validation set)* **do**

1. Fit a signature regression model as outlined in Algorithm 1.
2. Evaluate the hidden data set with the regression model.
3. Store predictions and errors.

end

end

Identify the best set of hyperparameters.

if *Recursive nowcasts* **then**

for *each time that a nowcast is required* **do**

1. Fit a signature regression model as outlined in Algorithm 1.
2. Evaluate the test set (only the time for the current nowcast) with the regression model for a nowcast value.

end

else

1. Combine the train and validation set and fit a signature regression model as outlined in Algorithm 1.
2. Evaluate the test set with the above trained regression model.

end

Return nowcast values.

gives the (transformed) observed values along with the true, hidden values that need to be inferred, as well as the predicted trajectories from the Kalman filter and the signature method.

B.1 Irregularly sampled data

Figure 11 shows how the residuals from the signature method compare to those from the Kalman filter for the case of irregular sampling.

The line of best fit shown in Figure 11 has gradient 0.93. The equivalent irregularly sampled inference of paths as in Figure 4 is shown in Figure 12: the signature method is able to provide a good approximation to the Kalman filter.

Figure 11: Residuals of the Kalman filter vs the signature method on irregularly sampled data. Marginal plots are histograms of residuals. The red line gives the line-of-best-fit.

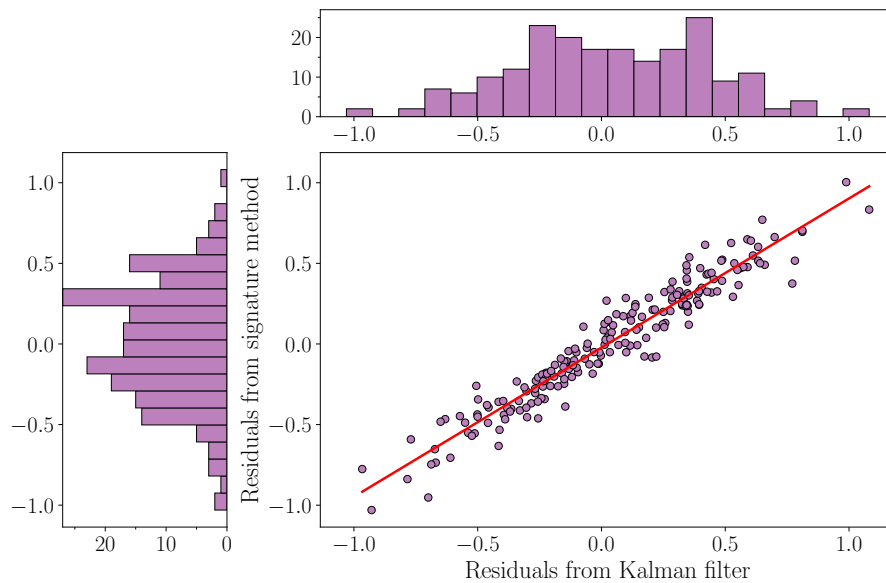
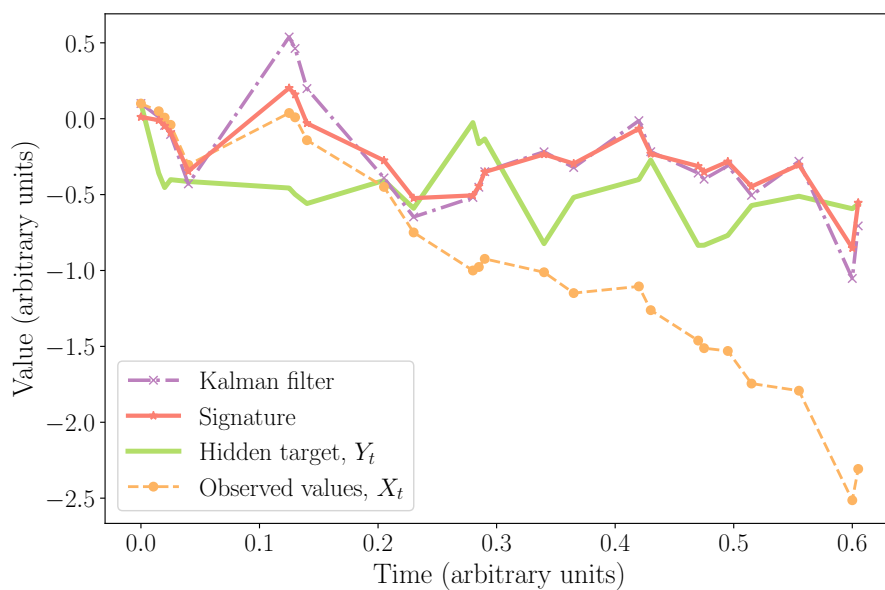


Figure 12: An *irregularly* sampled simulated path with observed values (X_t) along with the true, hidden values that need to be inferred (Y_t).



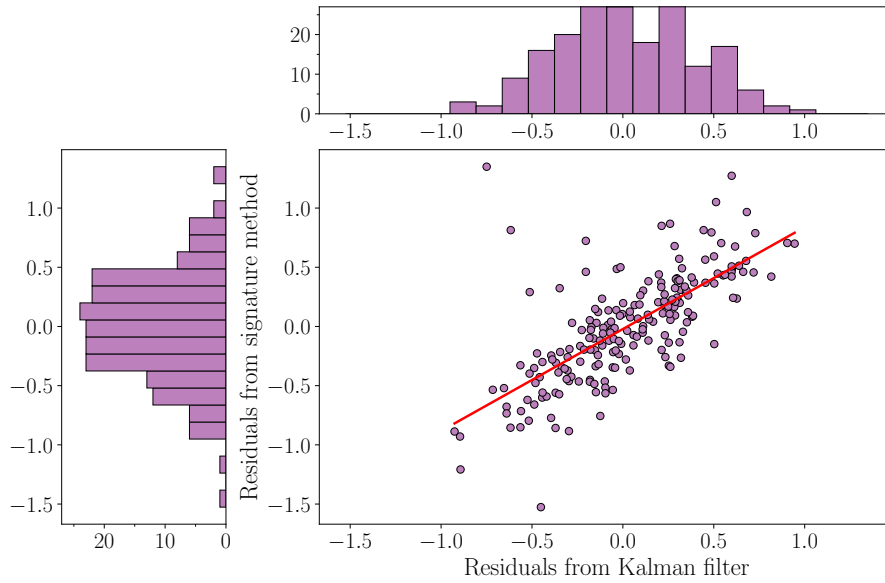
The simulation demonstrates that regression on signatures is a competitive method to infer

parameters even when data are not regularly sampled. No additional modifications need be made to the signature method to achieve this.

B.2 Non-linear data generating process

We use a sigmoid transform on the same regularly sampled trajectory data as in Figures 4 and 12. This transform allows the (theoretically optimal) Kalman filter to be derived in this non-linear context, for the sake of comparison. The residual comparison is in Figure 13, while the inferred paths are in Figure 14.

Figure 13: Residuals of the Kalman filter vs the signature method on data generated by a non-linear process. Marginal plots are histograms of residuals. The red line gives the line-of-best-fit.



B.3 Non-linear with irregularly sampled data

Figure 15 shows the comparison of the residuals, which is much weaker in this case. In Figure 16, we plot the results on the same simulated path as in Figure 14 but with observations that have been irregularly sampled. Despite the weaker correlation between the signature method residuals and the Kalman filter residuals, the predictions are not dissimilar.

C Configurations for nowcasting pipeline

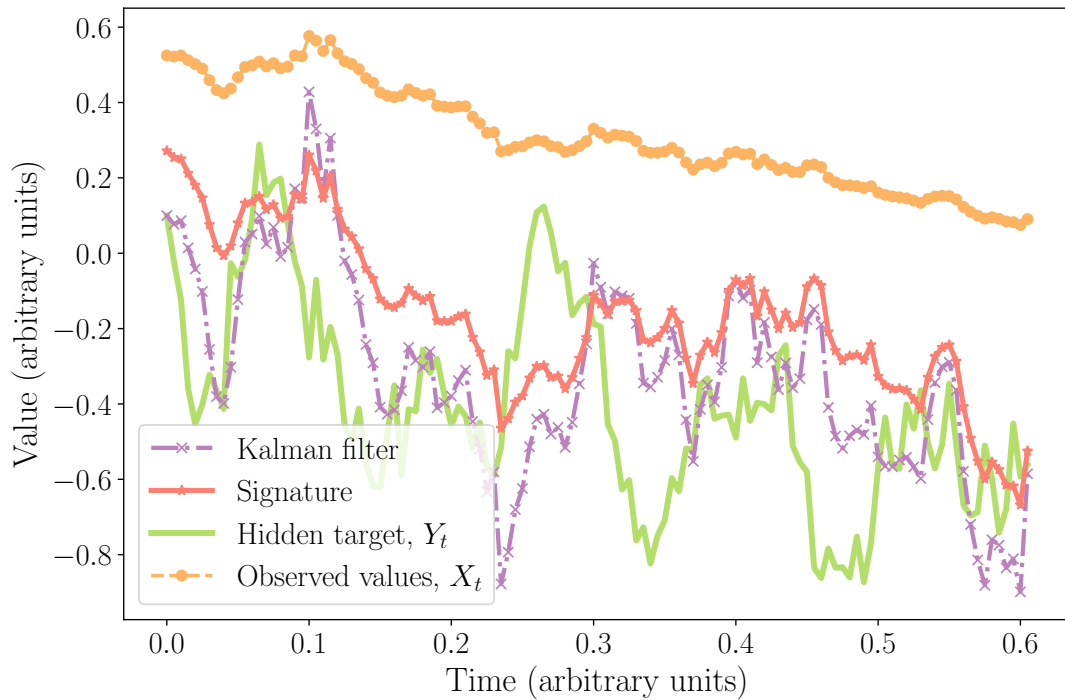
A short description of the main configuration settings for our signature nowcast can be found in Table 3.

In addition, the pipeline includes the possibilities to use custom factor structures to find principal components and much more. See the implementation of the experiments in this paper from our [Github repository](#) or refer to the documentation of our package [SigNow](#) for more details.

Table 3: Description of the main configs used in the nowcasting pipeline.

Parameter	Data Type	Description
window_type	str	The type of window used for generating the signatures - possible values are ‘days’, ‘ind’ and None. Arguments ‘days’ and ‘ind’ behave as moving windows. None acts as a expanding window.
max_length	int	When ‘window_type’ is set to ‘days’ or ‘ind’, ‘max_length’ is the number of days or rows to index by.
fill_method	str	How missing data should be filled - typical values ‘ffill’, ‘bfill’ or ‘rectilinear’.
level	int	Truncation level for the variables.
t_level	int	Truncation level for the time parameter.
basepoint	bool	Whether to add a basepoint of zeros before computing signatures to remove lateral invariance.
use_multiplier	bool	Whether to multiply only the signatures corresponding to time only by multiplier based on target series.
keep_sigs	str	The type of signature terms to keep - values ‘all’, ‘innermost’, ‘all_linear’ and None.
regularize	str	Method to regularize, accepted values are ‘elastic_net’, ‘l1’, ‘l2’, and None. Default: ‘elastic_net’.
alpha	float	Determines the strength of regularisation, see sklearn .
l1_ratio	float	Weight for the L1 penalty in the Elastic-Net of sklearn .
fit_intercept	bool	Whether to fit an intercept in regression.
target_lag	int	The target variable will have a lag due to the release timetable, this variable creates a shift so models never utilise future information.
use_prev_value	bool	Whether to use the latest value of the target series for the regression.
standardize	bool	Standardize signature terms before regression. Default: True.
training_proportion	float	This is an optional parameter to specify a fixed proportion for the train set.
reduce_dim	bool	Whether to reduce the dimension of the observed variables with principal component analysis.
k	int	The number of principal components to use.

Figure 14: Illustration of the same simulated path as in Figure 4 but now the observed data have been passed through a sigmoid transform.



Notes. The plot gives the transformed observed values along with the true, hidden values that need to be inferred, as well as the predicted trajectories from the Kalman filter and the signature method.

Figure 15: Residuals of the Kalman filter vs the signature method on data generated by a non-linear process and downsampled. Marginal plots are histograms of residuals. The red line gives the line-of-best-fit.

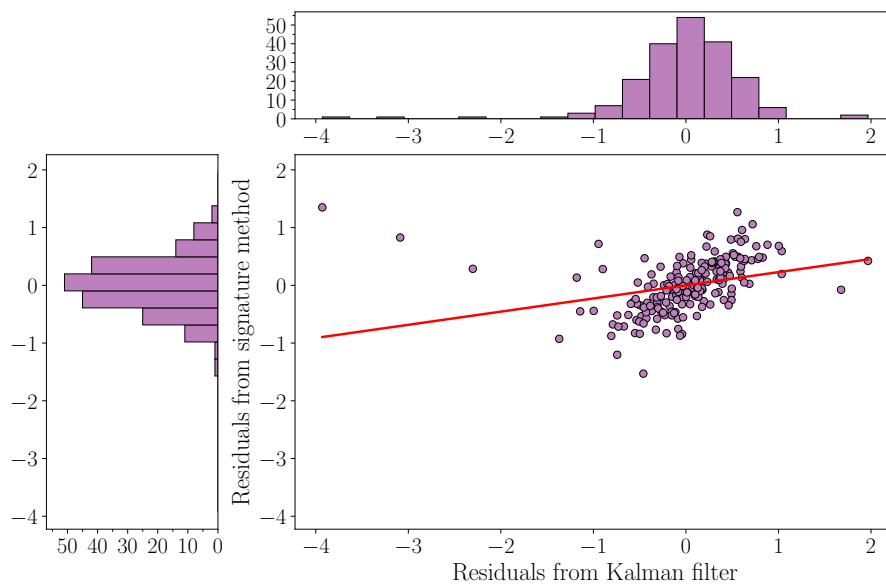
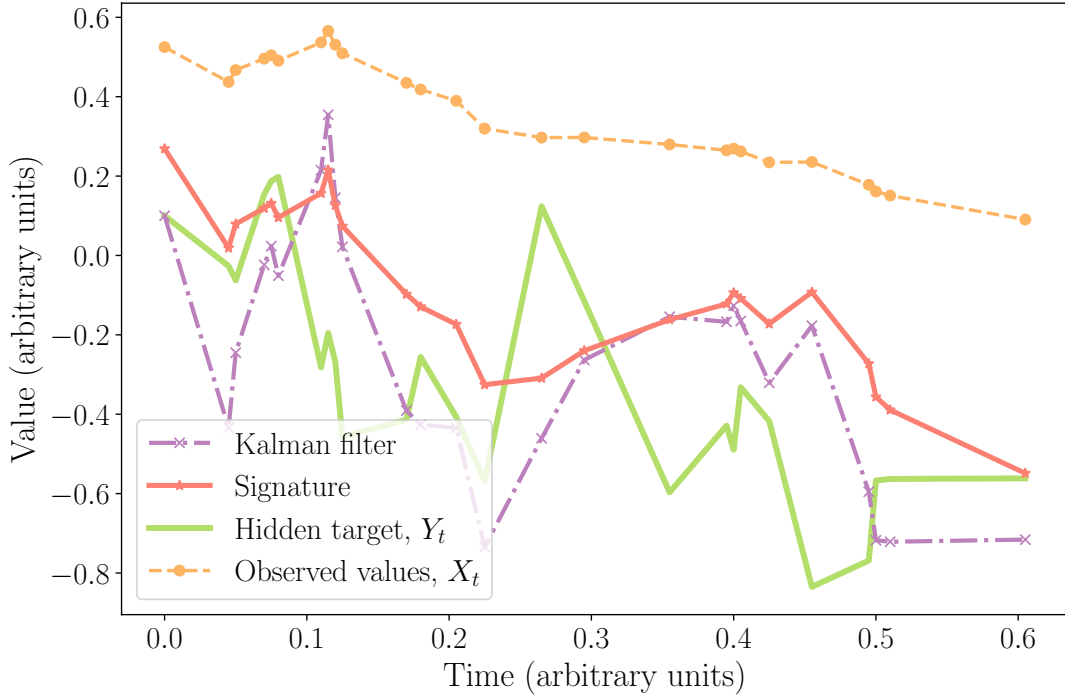


Figure 16: Illustration of the same simulated path as in Figure 14 (that is, after a sigmoid transform) but now irregularly sampled.



D Factor structure for the US GDP DFM

As in Bok et al. (2018), we assume that there are 4 factors labelled as soft, real, labour, and global which affect the time series behind the US GDP nowcasting application. In this appendix, we list the groupings. The global factor includes all variables (i.e. it contains factors in soft, real, and labour as well). The final list below, “other”, lists all the variables which do not fall under soft, real, and labour, and so are affected by the global factor alone.

Soft = {Empire state Mfg. Survey: General business conditions, Philly Fed Mfg. business outlook: Current activity, University of Michigan: Consumer Sentiment}

Real = {Real domestic gross product, Manufacturers new orders: Durable goods, Retail sales and food services, New single family houses sold, Housing starts, Industrial production index, Merchant wholesalers: Inventories: Total, Value of construction put in place, Building permits, Capacity utilization, Inventories: Total business, Real personal consumption expenditures, Manufacturing shipments: Durable goods, Mfrs. unfilled orders: All manufacturing industries, Manufacturing inventories: Durable goods, Real gross domestic income, Real disposable personal income, Exports: Goods and services, Imports: Goods and services}

Labour = {All employees: Total nonfarm, Civilian Unemployment rate, ADP nonfarm private payroll employment, Nonfarm business sector: Unit labor cost, JOLTS: Job openings: Total}

Other = {CPI-U: All items, PPI: Final demand, Import price index, PCE less food and energy: Chain price index, CPI-U: All items less food and energy, PCE: Chain price index, Export price

index}

E Experimental Details

E.1 US GDP

For the US GDP growth example, there are two models, depending on whether the data used are the principal components of each factor group, or whether they are the final hidden factors from the dynamic factor model.

The target variable has a 30 day publication lag after the end of the quarter. This corresponds to a lag of about 124 days from the start of the reference quarter. All signature terms are standardised as discussed in Section 4.2.

For the data obtained using PCA, the final fitted model used all the linear signature terms truncated at level 3 over a lookback window of 730 days. This is a ridge model with a regularisation parameter strength of 2.0. We use the previous value of the target in the regression and allow an intercept. We use the target series as a multiplier as seen in equation (11) but we do not append a basepoint to the start of the series (this is where a value, often 0, is appended to remove the lateral invariance) when computing the signatures. Missing data is filled by forward fill (carry the last value forward until another observation is made). A summary of these hyperparameters can be found in Table 4.

Table 4: Table of hyperparameters used to obtain the US GDP results with PCA “factors”.

Parameter	Value
level	3
t_level	3
fill_method	ffill
max_length	730
keep_sigs	all_linear
regularize	elasticnet
alpha	2.0
l1_ratio	0
standardize	True
fit_intercept	True
use_multiplier	True
basepoint	False
target_lag	124
use_prev_value	True

For the data obtained using DFM means as observations, the final fitted model again used all the linear signature terms truncated at level 3 over a lookback window of 730 days. This is a ridge model with a regularisation parameter strength of 1.0. We use the previous value of the target in the regression and allow an intercept. We use the target series as a multiplier but we do not use a basepoint when computing the signatures. Missing data is filled by rectilinear interpolation. A summary of these hyperparameters can be found in Table 5.

E.2 Nowcasting UK unemployment hyperparameters

The list of hyperparameters selected for nowcasting the UK unemployment can be found in Table 6.

F Consistency of signature regression

The consistency of the signature regression approach is somewhat delicate, as it naturally involves a high dimensional and possibly ill-posed estimation problem. In this appendix, we will outline what can easily be said about the statistical properties of our method, and give references to where these questions are pursued further in the literature.

Our approach will involve decomposing the errors of predictions into different sources, and showing that each of these can be made small, under appropriate assumptions. We will not give a formal statement of consistency (as this would involve heavy assumptions), but will indicate what would be involved in establishing such a result.

We will require some additional notation in order to perform these decompositions. We recall that \mathcal{F}_t^X is the σ -algebra describing the information available at time t from observations of X up to time t . We write $\mathcal{F}_{[t-\tau, t]}^X = \sigma(\{X_s\}_{s \in [t-\tau, t]})$ for the σ -algebra of information available from observations of X between times $t - \tau$ and t , and $\mathcal{S}_{[t-\tau, t]}^k(X)$ for the k th level signature of the augmented process (t, X_t) between times $[t - \tau, t]$. We write $L^*(Y_{t-}, \mathcal{S}_{[t-\tau, t]}^k(X))$ for the optimal (i.e. variance minimising) regression estimate when approximating Y as a linear function of Y_{t-} and $\mathcal{S}_{[t-\tau, t]}^k(X)$. Finally, we write $\hat{Y}_t = \hat{L}(Y_{t-}, \mathcal{S}_{[t-\tau, t]}^k(X))$ for the regression estimate we obtain using the method described in Section 4.

We now observe that we can decompose of the mean square error of our estimate as follows (noting that by the orthogonality of conditional-expectation, the first two decompositions do not introduce cross-terms, and the factor 2 arises from Young's inequality):

$$\begin{aligned} \mathbb{E}[(Y - \hat{Y})^2] &\leq \mathbb{E}\left[(Y - \mathbb{E}[Y|\mathcal{F}_t^X, Y_{t-}])^2\right] + \mathbb{E}\left[(\mathbb{E}[Y|\mathcal{F}_t^X, Y_{t-}] - \mathbb{E}[Y|\mathcal{F}_{[t-\tau, t]}^X, Y_{t-}])^2\right] \\ &\quad + 2\mathbb{E}\left[(\mathbb{E}[Y|\mathcal{F}_{[t-\tau, t]}^X, Y_{t-}] - L^*(Y_{t-}, \mathcal{S}_{[t-\tau, t]}^k(X)))^2\right] \\ &\quad + 2\mathbb{E}\left[(L^*(Y_{t-}, \mathcal{S}_{[t-\tau, t]}^k(X)) - \hat{Y}_t)^2\right]. \end{aligned}$$

We will address each of these terms in turn.

F.1 Unavoidable error

The quantity

$$\mathbb{E}\left[(Y - \mathbb{E}[Y|\mathcal{F}_t^X, Y_{t-}])^2\right]$$

is the unavoidable error of the estimation problem. This cannot be reduced using any mathematical or statistical technique, but is intrinsic to the information available. For this reason we focus on the subsequent errors.

F.2 Horizon-induced error

The quantity

$$\mathbb{E}\left[\left(\mathbb{E}[Y|\mathcal{F}_t^X, Y_{t-}] - \mathbb{E}[Y|\mathcal{F}_{[t-\tau, t]}, Y_{t-}]\right)^2\right]$$

represents the error induced by restricting our attention to a finite horizon/lookback window. Suppose we know that Y is a Markov process, and assume that Y_{t-} (which is an observation of Y at the most recent point prior to time t) comes from an observation time in the interval $[t - \tau, t]$. Then, by standard properties of Markov processes, we know that Y is conditionally independent of $\mathcal{F}_{t-\tau}^X$ given Y_{t-} . Recalling that $\mathcal{F}_t^X = \mathcal{F}_{t-\tau}^X \vee \mathcal{F}_{[t-\tau, t]}^X$, we conclude that this error is zero when Y is a Markov process and τ is sufficiently large relative to the delay in (true) observations of Y .

If we do not wish to assume that Y is Markov, or wish to exclude previous observations of Y , then this error can be controlled by studying the horizon dependence and ergodic properties of the filter estimate $\mathbb{E}[Y|\mathcal{F}_{[t-\tau, t]}]$. This is a well-studied problem, see for example van Handel (2014), Chigansky and Liptser (2004), Cohen and Fausti (2023) and references therein. However, the assumptions under which one can prove bounds on the horizon dependence are generally moderately restrictive.

F.3 Signature-approximation error

The quantity

$$\mathbb{E}\left[\left(\mathbb{E}[Y|\mathcal{F}_{[t-\tau, t]}^X, Y_{t-}] - L^*(Y_{t-}, \mathcal{S}_{[t-\tau, t]}^k(X))\right)^2\right]$$

represents the error due to approximating the conditional expectation as a linear function of the k th level signature. Proving bounds on this approximation error is an active area of mathematical research. The challenge here is to ensure that the map $X \rightarrow \mathbb{E}[Y|\mathcal{F}_{[t-\tau, t]}^X, Y_{t-}]$ is continuous in an appropriate sense. If we assume that our observation process X is in discrete time, and that the joint process (X, Y) has some minor level of regularity (for example, it would be sufficient if the vectors $\{X_{t_i}, Y_{t_i}\}_{i=1}^N$ have a joint density), then we can ensure this continuity. Consequently, the classical universal approximation theorem (see Levin et al. (2013)) applies, which guarantees we can approximate the conditional expectation arbitrarily well with high probability. More recent results (Cuchiero et al., 2025; Ceylan and Prömel, 2025) show precisely that the variance of this approximation can be made arbitrarily small, by using a sufficient number of signature terms.

The assumption of linearity in Y_{t-} is not a concern if the true relationship is linear, otherwise this potentially introduces another error in the model. To alleviate this error, one can simply use a richer regression family (for example, polynomial regression, splines, or other nonparametric methods). From this perspective, the assumption on linearity in Y_{t-} is not intrinsic to the signature regression model.

F.4 Regression error

The quantity

$$\mathbb{E}\left[\left(L^*(Y_{t-}, \mathcal{S}_{[t-\tau, t]}^k(X)) - \hat{Y}_t\right)^2\right]$$

represents the error due to the use of regression estimates based on a finite training sample.

The error due to regression can now be treated as in a standard regression problem. Observe that we have reduced the problem to a standard finite-dimensional regression problem, for which there is a well-established literature. We outline some primary concerns below.

Regression error with independent observations If we assume that we have access to a sequence of training paths, which are independently sampled, then we are in a standard regression setting. The consistency follows from the standard properties of linear regression where, as the sample size increases, the estimated regression coefficients converge to the coefficients in the best linear approximation. Classic results in this direction can be found in (Drygas, 1971, 1976; Amemiya, 1985), and the basic result on consistency of regression estimators is taught in most undergraduate courses in statistics and econometrics.

The presence of collinearity in the signature terms does raise some concerns here. Certain terms in the signature are guaranteed to satisfy quadratic shuffle identities (for example, the relationships $S^2(tx) + S^2(xt) = S^1(t)S^1(x)$ and $S^2(tt) + S^2(tx) + S^2(xt) + S^2(xx) = 1/2(S^1(t) + S^1(x))^2$ are illustrated in Figure 2), and so the regression technique needs to be modified to deal with this issue. Whether this is a practical concern depends on the interpretation of these coefficients – as the signature is guaranteed to satisfy these relationships, the ‘true’ coefficients are somewhat meaningless, as the model is not fully identifiable (but the predictions from the model are unique, both in and out-of sample). As the primary concern of these techniques is the model predictions, rather than the interpretation of specific coefficients of individual signature terms, this limitation has few consequences.

In the algorithm presented above, the regression problem is perturbed away from OLS methods by including a regularization term, yielding the regularised least-squares problem, which is strictly convex and hence has a unique optimizer. This may introduce a small amount of bias in the estimation procedure, but the standard results on the ridge regression will apply (see, for example, Hsu et al. (2012)).

We also consider an alternative solution, where we include only the ‘linear signature’ terms, i.e. where time is the only coefficient that is permitted to appear more than once in the signature. This lessens the problem of collinearity, provided we use data with a range of time horizons. The drawback of this restriction is that it forces a linear relationship to hold between the hidden target variable and the observation paths, which may be inappropriate in some contexts. We see that this assumption naturally arises in Section 3.6, which is based on classical (linear) Kalman filtering.

Regression error with dependent observations As discussed above, the fact that our method reduces to classical linear regression enables easy extension from the traditional setting

where we have access to independent observation paths, and allows more natural time-series assumptions to be made instead.

A classic extension is to assume that our observations are from an ergodic process, for which the use of a single long trajectory results in estimates that converge to their underlying averages. In particular, Lucchese et al. (2025) shows that under the assumption that our observation process is strongly mixing, the signature of our observations will also be strongly mixing (curiously, they also demonstrate that simply assuming ergodicity of the observation process is not sufficient to guarantee ergodicity of its signature). They then show the consistency of the sample average signature using non-overlapping intervals (along with central limit theorems for these quantities).

In a regression context, this implies that, under the assumption that our observations X and hidden target Y are (jointly) strongly mixing, the regularized regression estimator will also be consistent¹⁵.

When we use overlapping intervals, the results we obtain do not fall neatly into the setting of Lucchese et al. (2025). However, we can consider the non-overlapping interval case as simply being the combination of a collection of correlated learning problems with non-overlapping intervals. As all these problems are consistent, we see that this does not cause significant difficulty for the theory.

Infill asymptotics A further asymptotic regime that could be considered, but is not the focus here, is the setting in which we obtain increasingly frequent observations of the same path. The consistency of the discrete-observation signatures as approximations of the continuous signature is also considered in Lucchese et al. (2025), where it is shown that, assuming the observation process is sufficiently regular (in particular, it can be seen as a ‘geometric rough path’), then the estimates are consistent, and convergence rates are given.

In practice, this is less critical a concern for our analysis, as we do not suppose that it is generally possible to monitor the observation variables with arbitrary frequency. This aligns with the view that the observation process is not under the direct control of the econometrician, but is determined by other factors (such as availability of survey data, frequency of corporate reporting, etc...). Nevertheless, it is reassuring to know that there is indeed a consistency result in this direction, particularly when observations in high-frequency are available.

¹⁵The fact that Lucchese et al. (2025) only shows consistency of the average signature is not a concern here, as Chen’s identity shows that products of signature terms are themselves signature terms. This allows us to expand the regression coefficient in terms of the joint signature of (X, Y) over each non-overlapping interval, and hence apply their result to see consistency.

References

- Aastveit, K. A., Ravazzolo, F., and Van Dijk, H. K. (2018). Combined density nowcasting in an uncertain economic environment. *Journal of Business & Economic Statistics*, 36(1):131–145.
- Almon, S. (1965). The distributed lag between capital appropriations and expenditures. *Econometrica*, 33(1):178–196.
- Almuzara, M., Baker, K., O’Keeffe, H., and Sbordone, A. (2023). The new york fed staff nowcast 2.0. *New York FED Staff Technical Paper*.
- Amemiya, T. (1985). *Advanced Econometrics*. Harvard University Press.
- Anesti, N., Galvao, A. B., and Miranda-Agrippino, S. (2022). Uncertain kingdom: Nowcasting gross domestic product and its revisions. *Journal of Applied Econometrics*, 37(1):42–46.
- Ankargren, S. and Jonéus, P. (2021). Simulation smoothing for nowcasting with large mixed-frequency vars. *Econometrics and Statistics*, 19:97–113.
- Babii, A., Ghysels, E., and Striaukas, J. (2021). Machine learning time series regressions with an application to nowcasting. *Journal of Business & Economic Statistics*, pages 1–23.
- Babii, A., Ghysels, E., and Striaukas, J. (2022). Machine learning time series regressions with an application to nowcasting. *Journal of Business & Economic Statistics*, 40(3):1094–1106.
- Bai, J. and Ng, S. (2008). Large dimensional factor analysis. *Foundations and Trends in Econometrics*, 3(2):89–163.
- Bain, A. and Crisan, D. (2008). *Fundamentals of Stochastic Filtering*. Stochastic Modelling and Applied Probability. Springer New York.
- Bañbura, M. and Modugno, M. (2014). Maximum likelihood estimation of factor models on datasets with arbitrary pattern of missing data. *Journal of Applied Econometrics*, 29(1):133–160.
- Baum, L. E. and Eagon, J. A. (1967). An inequality with applications to statistical estimation for probabilistic functions of Markov processes and to a model for ecology. *Bulletin of the American Mathematical Society*, 73(3):360 – 363.
- Baum, L. E. and Petrie, T. (1966). Statistical inference for probabilistic functions of finite state markov chains. *The Annals of Mathematical Statistics*, 37(6):1554–1563.
- Baum, L. E., Petrie, T., Soules, G., and Weiss, N. (1970). A Maximization Technique Occurring in the Statistical Analysis of Probabilistic Functions of Markov Chains. *The Annals of Mathematical Statistics*, 41(1):164 – 171.
- Bergstrom, A. (1984). *Handbook of Econometrics*, volume 2, chapter 20 Continuous Time Stochastic Models and Issues of Aggregation over Time, pages 1145–1212. Elsevier Science Publisher.
- Bertsekas, D. P. (2012). *Dynamic Programming and Optimal Control*. Athena Scientific, 4th edition.
- Black, E., Wang, Z., Fredrikson, M., and Datta, A. (2021). Consistent counterfactuals for deep models. *arXiv preprint arXiv:2110.03109*.

- Bleistein, L., Fermanian, A., Jannot, A.-S., and Guilloux, A. (2023). Learning the dynamics of sparsely observed interacting systems. *arXiv*, abs/2301.11647.
- Bok, B., Caratelli, D., Giannone, D., Sbordone, A. M., and Tambalotti, A. (2018). Macroeconomic nowcasting and forecasting with big data. *Available at SSRN 3102227*.
- Broyden, C. G. (1970). The convergence of a class of double-rank minimization algorithms. *Journal of the Institute of Mathematics and Its Applications*, 6(1):76–90.
- Buccheri, G., Bormetti, G., Corsi, F., and Lillo, F. (2021). A score-driven conditional correlation model for noisy and asynchronous data: An application to high-frequency covariance dynamics. *Journal of Business & Economic Statistics*, 39(4):920–936.
- Byrd, R. H., Lu, P., Nocedal, J., and Zhu, C. (1995). A limited memory algorithm for bound constrained optimization. *SIAM Journal on Scientific Computing*, 16(5):1190–1208.
- Carriero, A., Galvao, A. B., and Kapetanios, G. (2019). A comprehensive evaluation of macroeconomic forecasting methods. *International Journal of Forecasting*, 35(4):1226–1239.
- Carter, C. K. and Kohn, R. (1994). On gibbs sampling for state space models. *Biometrika*, 81(3):541–553.
- Ceylan, M. and Prömel, D. (2025). Universality of signature models. *In preparation*.
- Chan, J. C., Poon, A., and Zhu, D. (2023). High-dimensional conditionally gaussian state space models with missing data. *Journal of Econometrics*, 236(1):105468.
- Chen, K.-T. (1954). Iterated integrals and exponential homomorphisms. *Proceedings of the London Mathematical Society*, 4(1):502–512.
- Chevryrev, I. and Kormilitzin, A. (2025). A primer on the signature method in machine learning. *arXiv*, abs/1603.03788.
- Chigansky, P. and Liptser, R. (2004). Stability of nonlinear filters in nonmixing case. *The Annals of Applied Probability*, 14(4):2038 – 2056.
- Cochrane, T., Foster, P., Chhabra, V., Lemercier, M., Salvi, C., and Lyons, T. (2021). SK-Tree: a systematic malware detection algorithm on streaming trees via the signature kernel. *arXiv*, abs/2102.07904.
- Cohen, S. and Elliott, R. (2015). *Stochastic Calculus and Applications*. Probability and Its Applications. Springer New York, 2nd edition.
- Cohen, S. N. and Fausti, E. (2023). Exponential contractions and robustness for approximate wonham filters.
- Cuchiero, C., Schmock, P., and Teichmann, J. (2025). Global universal approximation of functional input maps on weighted spaces. *arXiv preprint arXiv:2306.03303*.
- Curtin, R. (2008). Consumer Sentiment Index. In Lavrakas, P. J., editor, *Encyclopedia of Survey Research Methods*, pages 136–138. Sage Publications, Inc., Thousand Oaks.
- Dempster, A. P., Laird, N. M., and Rubin, D. B. (1977). Maximum likelihood from incomplete data via the em algorithm. *Journal of the Royal Statistical Society. Series B (Methodological)*, 39(1):1–38.

- Doz, C., Giannone, D., and Reichlin, L. (2006). A quasi maximum likelihood approach for large approximate dynamic factor models. *European Central Bank Working paper No. 674/September 2006*.
- Drygas, H. (1971). Consistency of the least squares and gauss-markov estimators in regression models. *Zeitschrift für Wahrscheinlichkeitstheorie und Verwandte Gebiete*, 17(4):309–326.
- Drygas, H. (1976). Weak and strong consistency of the least squares estimators in regression models. *Zeitschrift für Wahrscheinlichkeitstheorie und Verwandte Gebiete*, 34(2):119 – 127.
- Durbin, J. and Koopman, S. J. (2012). *Time series analysis by state space methods*, volume 38. OUP Oxford.
- Fermanian, A. (2020). Linear functional regression with truncated signatures. *arXiv:2006.08442*.
- Fermanian, A. (2021). Embedding and learning with signatures. *Computational Statistics & Data Analysis*, 157:107148.
- Fletcher, R. (1970). A new approach to variable metric algorithms. *The Computer Journal*, 13(3):317–322.
- FRBNY (2016). Nowcasting report.
- Friz, P. and Hairer, M. (2020). *A Course on Rough Paths: With an Introduction to Regularity Structures*. Universitext. Springer International Publishing.
- Geweke, J. (1977). *The dynamic factor analysis of economic timeseries models*. In: *Latent variables in socio-economic models*. Amsterdam: North-Holland Publishing Company.
- Ghysels, E., Santa-Clara, P., and Valkanov, R. (2005). There is a risk-return trade-off after all. *Journal of financial economics*, 76(3):509–548.
- Giannone, D., Reichlin, L., and Small, D. H. (2006). Nowcasting gdp and inflation: the real-time informational content of macroeconomic data releases. *European Central Bank Working paper No. 633/May 2006*.
- Giusti, C. and Lee, D. (2020). Iterated integrals and population time series analysis. In Baas, N. A., Carlsson, G. E., Quick, G., Szymik, M., and Thaule, M., editors, *Topological Data Analysis*, pages 219–246, Cham. Springer International Publishing.
- Goldfarb, D. (1970). A family of variable-metric methods derived by variational means. *Mathematics of Computation*, 24(109):23–26.
- Graham, B. (2013). Sparse arrays of signatures for online character recognition. *arXiv*, abs/1308.0371.
- Gu, H., Guo, X., Jacobs, T. L., Kaminsky, P., and Li, X. (2024). Transportation marketplace rate forecast using signature transform. In *Proceedings of the 30th ACM SIGKDD Conference on Knowledge Discovery and Data Mining*, pages 4997–5005.
- Gyurkó, L. G., Lyons, T., Kontkowski, M., and Field, J. (2013). Extracting information from the signature of a financial data stream. *arXiv*.
- Hambly, B. and Lyons, T. (2010). Uniqueness for the signature of a path of bounded variation and the reduced path group. *Annals of Mathematics*, 171(1):109–167.
- Hamilton, J. D. (1994). State-space models. *Handbook of Econometrics*, 4:3039–3080.

- Harvey, A. C. (1990). *Forecasting, Structural Time Series Models and the Kalman Filter*. Cambridge University Press.
- Hoerl, A. E. and Kennard, R. W. (1970). Ridge regression: Biased estimation for nonorthogonal problems. *Technometrics*, 12(1):55–67.
- Hsu, D., Kakade, S. M., and Zhang, T. (2012). Random design analysis of ridge regression. In *Conference on learning theory*, pages 9–1. JMLR Workshop and Conference Proceedings.
- Jazwinski, A. H. (1970). *Stochastic Processes and Filtering Theory*, volume 64 of *Mathematics in Science and Engineering*. Academic Press, New York and London.
- Jokubaitis, S., Celov, D., and Leipus, R. (2021). Sparse structures with lasso through principal components: Forecasting gdp components in the short-run. *International Journal of Forecasting*, 37(2):759–776.
- Kalman, R. E. (1960). A New Approach to Linear Filtering and Prediction Problems. *Journal of Basic Engineering*, 82(1):35–45.
- Karlsson, S. (2013). Forecasting with bayesian vector autoregression. *Handbook of economic forecasting*, 2:791–897.
- Kim, C.-J. (1994). Dynamic linear models with markov-switching. *Journal of Econometrics*, 60(1-2):1–22.
- Kim, C.-J., Nelson, C. R., et al. (1999). State-space models with regime switching: classical and gibbs-sampling approaches with applications. *MIT Press Books*, 1.
- Kloeden, P. E. and Platen, E. (1992). *Numerical Solution of Stochastic Differential Equations*, volume 23 of *Stochastic Modelling and Applied Probability*. Springer-Verlag, Berlin/ Heidelberg, 1st edition.
- Levin, D., Lyons, T., and Ni, H. (2013). Learning from the past, predicting the statistics for the future, learning an evolving system. *arXiv*.
- Litterman, R. (1979). Techniques of forecasting using vector autoregressions. Technical report, Federal Reserve Bank of Minneapolis.
- Lucchese, L., Pakkanen, M. S., and Veraart, A. E. D. (2025). Learning with expected signatures: Theory and applications. In *Forty-second International Conference on Machine Learning*.
- Lundberg, S. M. and Lee, S.-I. (2017). A unified approach to interpreting model predictions. *Advances in neural information processing systems*, 30.
- Lyons, T., Ni, H., and Oberhauser, H. (2014). A feature set for streams and an application to high-frequency financial tick data. In *Proceedings of the 2014 International Conference on Big Data Science and Computing*, BigDataScience '14, New York, NY, USA. Association for Computing Machinery.
- Lyons, T. J., Caruana, M., and Lévy, T. (2007). *Differential Equations Driven by Rough Paths*. Springer.
- McCracken, M. W. and Ng, S. (2016). Fred-md: A monthly database for macroeconomic research. *Journal of Business & Economic Statistics*, 34(4):574–589.

- Morley, S. and Lyons, T. (2024). Roughpy. In *Proceedings of the 23rd Python in Science Conference*.
- Morrill, J., Fermanian, A., Kidger, P., and Lyons, T. (2021a). A Generalised Signature Method for Multivariate Time Series Feature Extraction. *arXiv*, abs/2006.00873.
- Morrill, J., Kidger, P., Yang, L., and Lyons, T. (2022). On the Choice of Interpolation Scheme for Neural CDEs. *Transactions on Machine Learning Research*.
- Morrill, J., Salvi, C., Kidger, P., Foster, J., and Lyons, T. (2021b). Neural rough differential equations for long time series. *International Conference on Machine Learning*.
- Morrill, J. H., Kormilitzin, A., Nevado-Holgado, A. J., Swaminathan, S., Howison, S. D., and Lyons, T. J. (2020). Utilization of the signature method to identify the early onset of sepsis from multivariate physiological time series in critical care monitoring. *Critical Care Medicine*, 48(10):e976–e981.
- Ni, H., Szpruch, L., Sabate-Vidales, M., Xiao, B., Wiese, M., and Liao, S. (2021). Sig-Wasserstein GANs for Time Series Generation. *arXiv*, abs/2111.01207.
- Nielsen, A. and Berg, C. W. (2014). Estimation of time-varying selectivity in stock assessments using state-space models. *Fisheries Research*, 158:96–101.
- Pedregosa, F., Varoquaux, G., Gramfort, A., Michel, V., Thirion, B., Grisel, O., Blondel, M., Prettenhofer, P., Weiss, R., Dubourg, V., et al. (2011). Scikit-learn: Machine learning in python. *Journal of Machine Learning Research*, 12(Oct):2825–2830.
- Pellegrino, F. (2020). Selecting time-series hyperparameters with the artificial jackknife. *arXiv preprint arXiv:2002.04697*.
- Proietti, T., Giovannelli, A., Ricchi, O., Citton, A., Tegami, C., and Tinti, C. (2021). Nowcasting gdp and its components in a data-rich environment: The merits of the indirect approach. *International Journal of Forecasting*, 37(4):1376–1398.
- Reizenstein, J. and Graham, B. (2020). Algorithm 1004: The iisignature library: Efficient calculation of iterated-integral signatures and log signatures. *ACM Transactions on Mathematical Software (TOMS)*.
- Richardson, A., van Florenstein Mulder, T., and Vehbi, T. (2021). Nowcasting gdp using machine-learning algorithms: A real-time assessment. *International Journal of Forecasting*, 37(2):941–948.
- Schumacher, C. (2016). A comparison of midas and bridge equations. *International Journal of Forecasting*, 32(2):257–270.
- Shanno, D. F. (1970). Conditioning of quasi-newton methods for function minimization. *Mathematics of Computation*, 24(111):647–656.
- Sims, C. A. (1980). Macroeconomics and reality. *Econometrica*, pages 1–48.
- Smeeke, S. and Wijler, E. (2021). An automated approach towards sparse single-equation cointegration modelling. *Journal of Econometrics*, 221(1):247–276.
- Soybilgen, B. and Yazgan, E. (2021). Nowcasting us gdp using tree-based ensemble models and dynamic factors. *Computational Economics*, 57(1):387–417.

- Stock, J. and Watson, M. (2017). *Dynamic Factor Models*. In: Clements MP, Henry DF Oxford *Handbook of Economic Forecasting*. Oxford University Press.
- Stock, J. H. and Watson, M. W. (2002). Forecasting using principal components from a large number of predictors. *Journal of the American Statistical Association*, 97(460):1167–1179.
- Tibshirani, R. (1996). Regression shrinkage and selection via the lasso. *Journal of the Royal Statistical Society: Series B (Methodological)*, 58(1):267–288.
- van Handel, R. (2014). *Ergodicity, Decisions, and Partial Information*, pages 411–459. Springer International Publishing, Cham.
- Wallis, K. F. (1986). Forecasting with an econometric model: The ‘ragged edge’ problem. *Journal of Forecasting*, 5(1):1–13.
- Wu, C. F. J. (1983). On the Convergence Properties of the EM Algorithm. *The Annals of Statistics*, 11(1):95 – 103.
- Yang, W., Lyons, T., Ni, H., Schmid, C., and Jin, L. (2017). Developing the path signature methodology and its application to landmark-based human action recognition. *arXiv: Computer Vision and Pattern Recognition*.
- Zou, H. and Hastie, T. (2005). Regularization and variable selection via the elastic net. *Journal of the Royal Statistical Society: Series B (Statistical Methodology)*, 67(2):301–320.

Table 5: Table of hyperparameters used to obtain the US GDP results with filtered DFM factors.

Parameter	Value
level	3
t_level	3
fill_method	rectilinear
max_length	730
keep_sigs	all_linear
regularize	elasticnet
alpha	1.0
l1_ratio	0
standardize	True
fit_intercept	True
use_multiplier	True
basepoint	False
target_lag	124
use_prev_value	True

Table 6: Table of hyperparameters used for nowcasting UK unemployment – see Section 7. Items in bold have been selected by tuning; otherwise we have chosen their values.

Parameter	Value
level	3
t_level	3
fill_method	rectilinear
max_length	40 days
keep_sigs	all_linear
regularize	elasticnet
alpha	0
l1_ratio	0
standardize	False
fit_intercept	True
use_multiplier	False
basepoint	True
target_lag	8
use_prev_value	True